Chapter I

Section C

Amine Functionalized Graphene Oxide Nanosheets (AFGONs): An Efficient Bifunctional Catalyst for the Synthesis of 1,4-Dihydropyridines

I.C.1 Introduction

Among the various six membered nitrogen heterocycles, 1,4-dihydropyridines (1,4-DHPs) are well known for their widespread activity in the field of medicinal chemistry.[1] 1,4-DHPs are privileged pharmacophore for multifarious marketed drugs.[1] This structural scaffold has attracted much attention owing to its diverse pharmaceutical and biological profile. They have remarkable pharmacological efficiency and are used as bronchodilators, vasodilators, anti-hypertensive, anti-diabetic, anti-inflammatory, anti-HIV, anti-tuberculosis agents and acts as chemosensitizer in tumour therapy.[2-7] 1,4-DHPs like nifedipine, amlodipine and nitrendipine have been used as clinical drugs for calcium channel blockers in the treatment of cardiovascular diseases.[8-11] Besides, some 1,4-DHPs are also associated with therapeutic properties like non-competitive inhibition of topoisomerase I and HIV protease inhibition.[12-17] 1,4-Dihydropyridines also possess cerebral anti-ischemic properties, which could find application in the treatment of Alzheimer's disease.[18] Certain 1,4-DHPs due to their close resemblance with NADH coenzyme are considered as bio mimetic agents in biological redox processes.[19-21] 1,4-Dihydropyridines also acts important intermediates during the preparation of several alkaloids.[22] In the field of transfer hydrogenation 1,4-DHPs are often used as sacrificial hydrogen source for the reduction of organic compounds containing different functional groups like C=O, C=N, C=C, etc.[23] Few representative bioactive molecules possessing functionalized 1,4-dihydropyridine unit that are in clinical use are shown in Figure I.C.1.

The synthesis of 1,4-dihydropyridines has been first reported by Arthur Hantzsch in 1882.[24] This classical method involves one-pot three-component condensation between aldehyde, ethyl acetoacetate and ammonia, either in acetic acid or under refluxing ethanol (Scheme I.C.1). Although, this approach based on multicomponent reaction (MCR) has been followed even today, it has certain limitations like low yield of product, prolong reaction time and harsh reaction conditions.

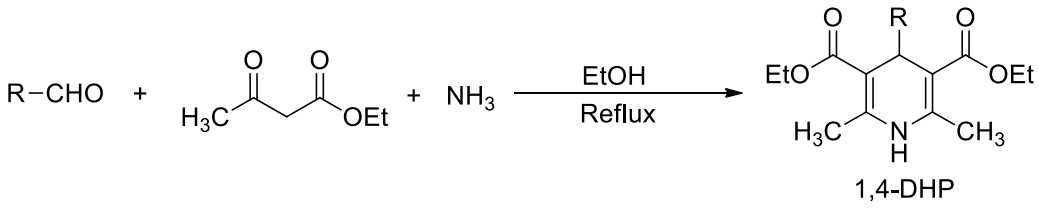

Scheme I.C.1 Classical three-component Hantzsch synthesis of 1,4-dihydropyridine.

I.C.1 Introduction

Among the various six membered nitrogen heterocycles, 1,4-dihydropyridines (1,4-DHPs) are well known for their widespread activity in the field of medicinal chemistry.[1] 1,4-DHPs are privileged pharmacophore for multifarious marketed drugs.[1] This structural scaffold has attracted much attention owing to its diverse pharmaceutical and biological profile. They have remarkable pharmacological efficiency and are used as bronchodilators, vasodilators, anti-hypertensive, anti-diabetic, anti-inflammatory, anti-HIV, anti-tuberculosis agents and acts as chemosensitizer in tumour therapy.[2-7] 1,4-DHPs like nifedipine, amlodipine and nitrendipine have been used as clinical drugs for calcium channel blockers in the treatment of cardiovascular diseases.[8-11] Besides, some 1,4-DHPs are also associated with therapeutic properties like non-competitive inhibition of topoisomerase I and HIV protease inhibition.[12-17] 1,4-Dihydropyridines also possess cerebral anti-ischemic properties, which could find application in the treatment of Alzheimer's disease.[18] Certain 1,4-DHPs due to their close resemblance with NADH coenzyme are considered as bio mimetic agents in biological redox processes.[19-21] 1,4-Dihydropyridines also acts important intermediates during the preparation of several alkaloids.[22] In the field of transfer hydrogenation 1,4-DHPs are often used as sacrificial hydrogen source for the reduction of organic compounds containing different functional groups like C=O, C=N, C=C, etc.[23] Few representative bioactive molecules possessing functionalized 1,4-dihydropyridine unit that are in clinical use are shown in Figure I.C.1.

The synthesis of 1,4-dihydropyridines has been first reported by Arthur Hantzsch in 1882.[24] This classical method involves one-pot three-component condensation between aldehyde, ethyl acetoacetate and ammonia, either in acetic acid or under refluxing ethanol (Scheme I.C.1). Although, this approach based on multicomponent reaction (MCR) has been followed even today, it has certain limitations like low yield of product, prolong reaction time and harsh reaction conditions.

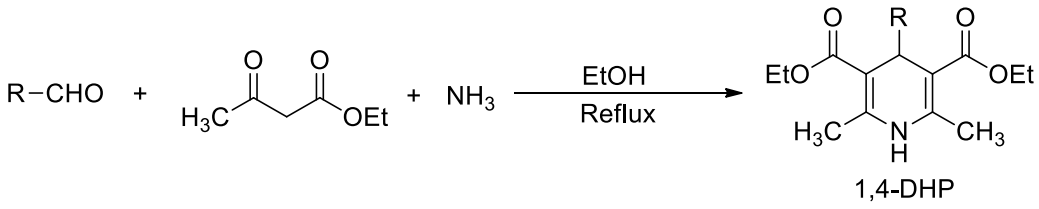

Scheme I.C.1 Classical three-component Hantzsch synthesis of 1,4-dihydropyridine.

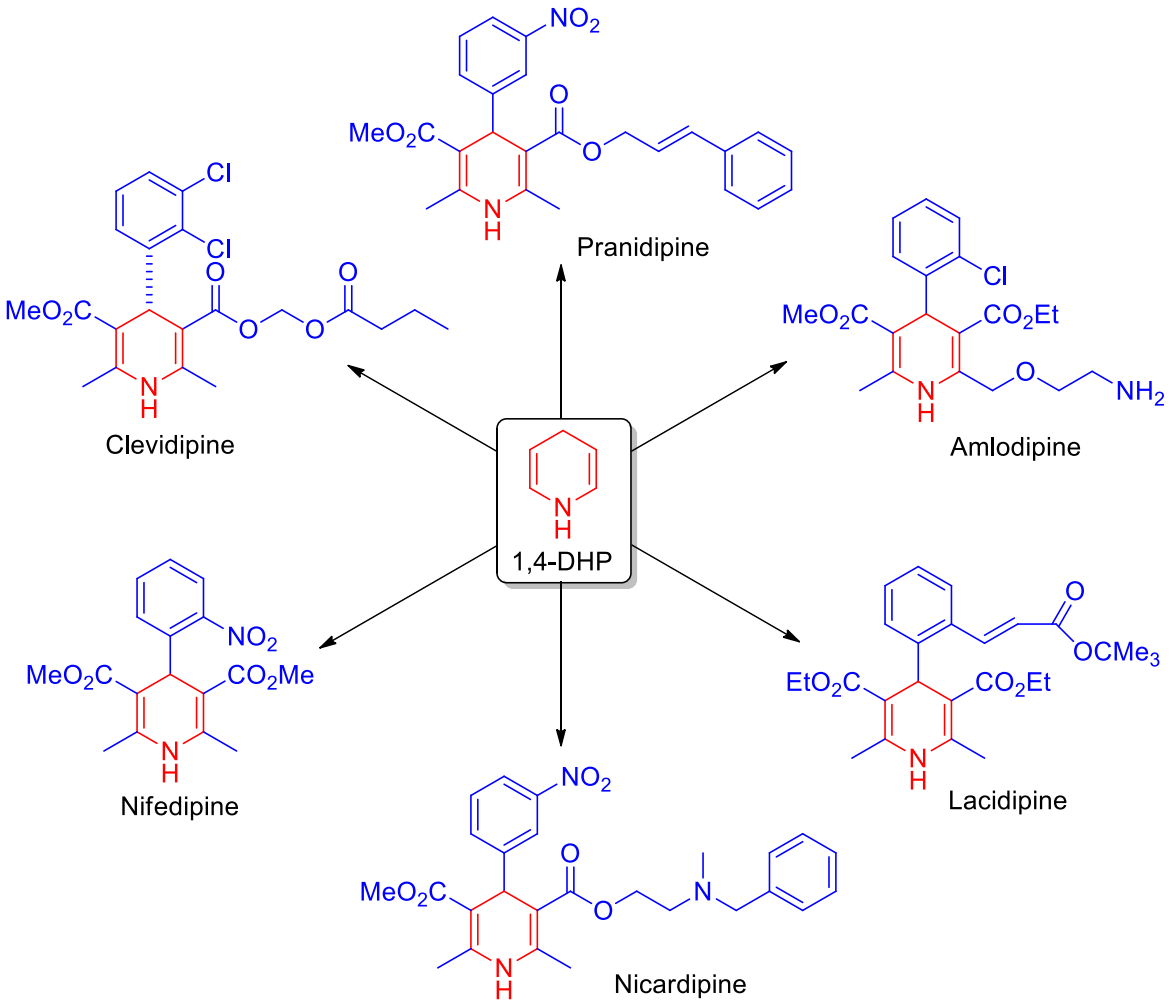

Figure I.C.1 Examples of clinical drugs bearing functionalized 1,4-dihydropyridine unit.

In the view of economical and environmental facets, organic synthesis that aims to maximize efficiency and minimize waste at source has been in demand recently. Although, myriads of new strategies have been developed, multicomponent reactions (MCRs) have emerged as an exceptional tool due to its remarkable synthetic efficiency, high atom economy, devoid of complex purification procedures, minimal waste generation and energy consumption.[25] MCRs can efficaciously enhance the reactivity of chemical processes and have been commonly used for the genesis of carbon-carbon and carbon-heteroatom bonds in a single step. Thus, MCRs allow direct and elegant access to library of complex structural diversity.

On the other hand, heterogeneous catalysts based on graphene and chemically modified graphenes (CMGs) have received prodigious attention owing to their potential for catalysis under benign conditions.[26] Moreover, functionalized graphenes possesses high surface area and diverse functionalities thereby facilitating catalytic performance.[27] Besides, such catalytic

systems could be easily re-used and provides a convenient and practical way to synthesize complex organic molecules.

I.C.2 Background and objectives

Owing to the limitations of the classical Hantzsch synthesis, innumerable strategies have been developed which attempts to improve the Hantzsch.[28] A wide range of homogeneous and heterogeneous catalysts have been employed for the synthesis of diverse 1,4-dihydropyridine derivatives.[29] Strong acids,[30,31] and silica based composites have been widely used as catalysts for the synthesis of 1,4-DHPs.[32,33] Apart from silica based composites various metal salts, metallic nanoparticles (NPs) and supported metal catalysts are also used as catalyst which often generates hazardous wastes thereby compromising environmental safety.[34-36] The use of magnetic nanocatalysts in Hantzsch synthesis renders easy removal of the catalyst after the reaction by using an external magnet.[37,38] Other commonly used catalytic systems for the synthesis of 1,4-DHPs include *p*-TSA,[39] montmorillonite clay,[40] sulfated polyborate,[41] zeolite,[42] chitosan NPs,[43] polyethylene glycol,[44] PPh_3,[45] ionic liquids (ILs),[46] heteropoly acids,[47] and organocatalysts.[48] Most of these procedures employ harsh reaction conditions, uses toxic solvents and requires tedious purification steps. The diverse strategies involved in the synthesis of 1,4-DHPs have been nicely presented in a review article by Wan and co-workers.[28] The following section represents few recent strategies involved in the synthesis of 1,4-DHPs.

Silica gel supported sodium bisulfate (SiO_2-$NaHSO_4$) has been prepared and used for the one-pot synthesis of 1,4-dihydropyridines at ambient temperature (Scheme I.C.2). Diverse 1,4-dihydropyridine derivatives were synthesized in good to excellent yields. The catalyst being heterogeneous in nature could be recycled and reused for further catalytic runs.[49]

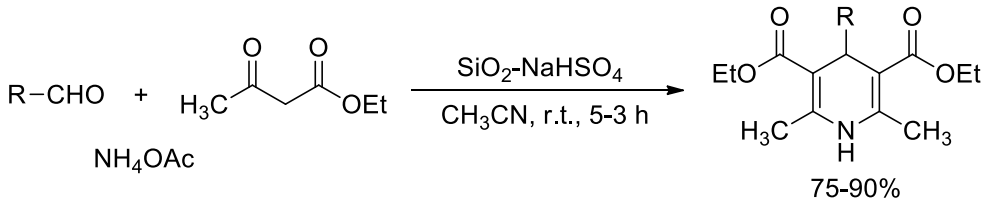

Scheme I.C.2 SiO_2-$NaHSO_4$ catalyzed synthesis of 1,4-dihydropyridines.

Kilbas and co-workers have prepared monodispersed Pd, Ru and Ni nanoparticles embedded on graphene oxide nanosheets by using double solvent reduction method under ultrasonication. The catalyst has been characterized by different spectroscopic techniques. The as-prepared nanocomposite (PdRuNi@GO) has been employed for the synthesis of 1,4-

dihydropyridines and hexahydroquinolines based on a multicomponent approach (Scheme I.C.3). The authors also suggested a plausible mechanism and checked recyclability of the catalyst for five cycles.[36]

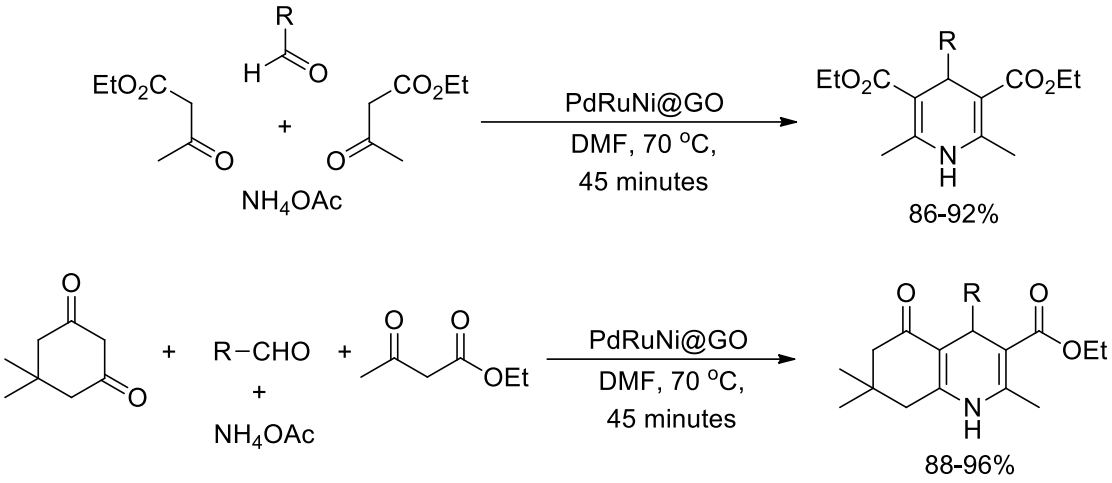

Scheme I.C.3 PdRuNi@GO catalyzed synthesis of 1,4-DHPs and hexahydroquinolines.

Zirconia supported sulfonic acid nanocomposite (n-ZrSA) has been prepared from nano zirconia by using chlorosulfonic acid. The material has been characterized in detail by spectroscopic techniques and used for four different multicomponent reactions. A wide range of hexahydroquinoline, 1,8-dioxo-decahydroacridine, polyhydroquinoline and 1,8-dioxo-octahydroxanthene derivatives were synthesized under solvent free conditions (Scheme I.C.4). The acidity strength of n-ZrSA has been determined by using Hammett acidity function and the acid capacities have been calculated by acid-base potentiometric titration.[30]

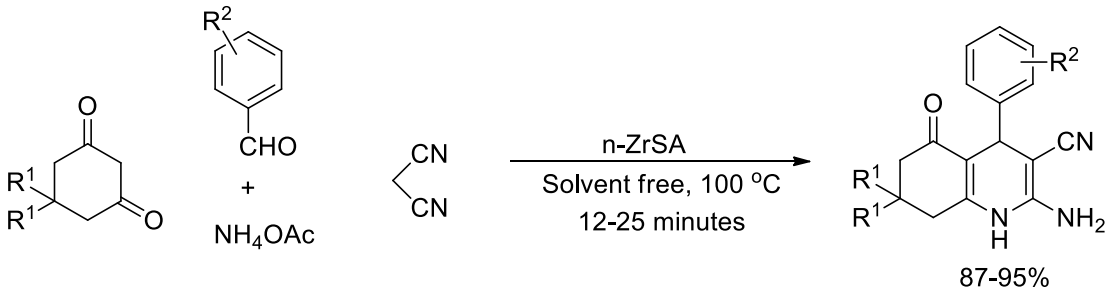

Scheme I.C.4 Zirconia sulfonic acid catalyzed synthesis of hexahydroquinolines.

An expedient synthesis of 1,4-dihydropyridines has been reported by using nano-Fe_2O_3 catalyst. The reaction conditions are facile and involve stirring of the reactants under solvent free conditions at 90 °C (Scheme I.C.5). The magnetic nature of the catalyst also facilitates easy recovery and recyclability. The investigators also proposed a mechanism where activation of the carbonyl group is facilitated by coordination with Fe^{3+} moiety.[38]

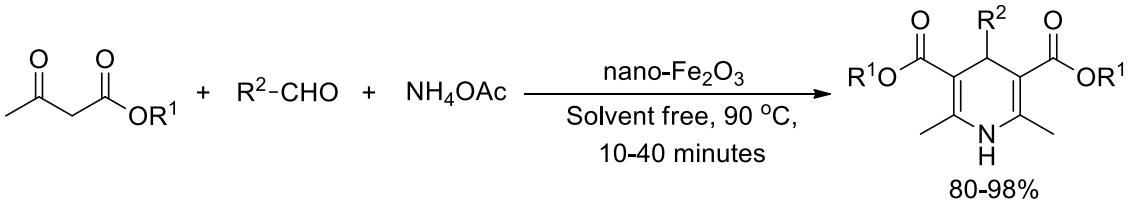

Scheme I.C.5 Three-component synthesis of 1,4-DHPs using nano-Fe_2O_3.

The synthesis of 1,4-DHPs has been accomplished by using sulfated polyborate as an efficient heterogeneous catalyst. The catalyst has been prepared from boric acid by dehydration followed by sulfonation using chlorosulfonic acid (Scheme I.C.6). The resulting material catalyzed the three-component reaction between β-ketoesters, aldehydes and ammonium carbonate under solvent free conditions.[41]

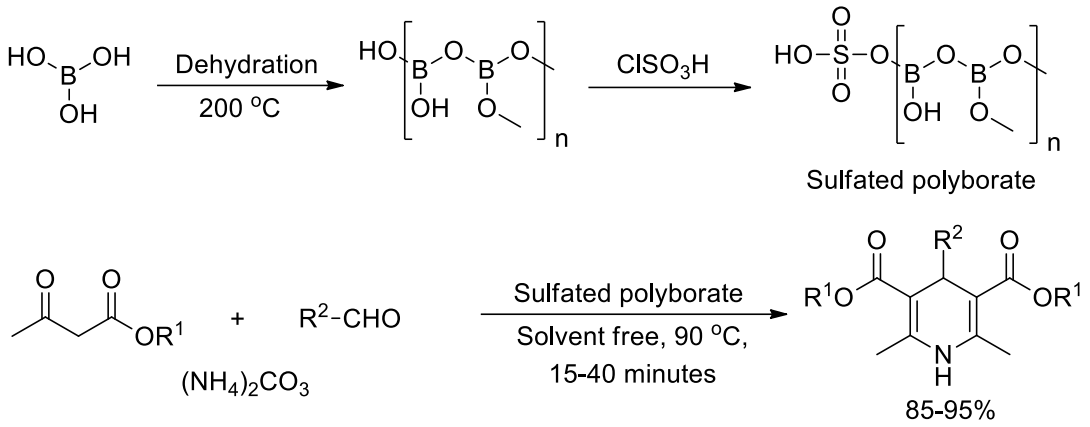

Scheme I.C.6 Synthesis of 1,4-DHPs using sulfated polyborate catalyst.

The synthesis of functionalized 1,8-dioxoacridines has been accomplished by using $Bi(NO_3)_3{\cdot}5H_2O$ at ambient temperature. A pseudo four-component reaction between 1,3-diketones, aldehydes and primary amines afforded the desired products in 63-99% yield (Scheme I.C.7). The authors proposed a plausible mechanism which initially involved Claisen-Schmidt condensation between 1,3-diketone and aldehyde catalyzed by Bi^{3+} ions.[34]

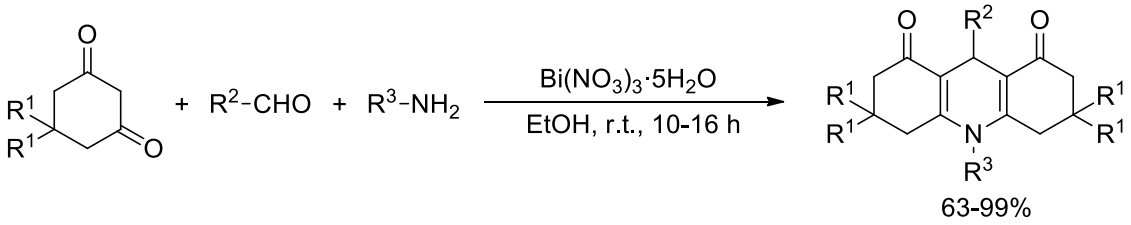

Scheme I.C.7 Bismuth nitrate catalyzed three-component synthesis of 1,8-dioxoacridines.

Ionic liquid catalyzed multicomponent synthesis of acridinediones has been reported by Zhu and co-workers.[46] A series of betainium based ionic liquid has been tested for their catalytic activity and betainium lactate [HBet][Lac] showed the highest activity (Scheme I.C.8). Moreover, the catalyst could be recycled for five runs without any loss in the yield of product. The investigators also proposed a plausible mechanism and showed the role of ionic liquid.

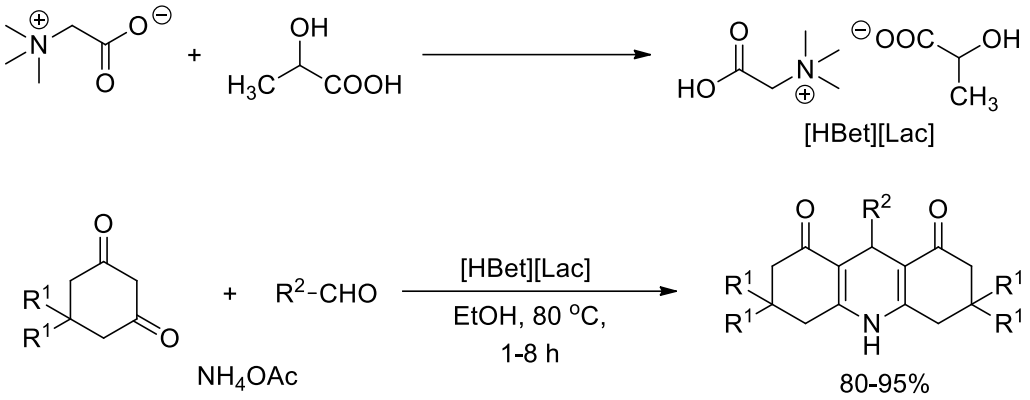

Scheme I.C.8 Betainium lactate catalyzed synthesis of acridinediones.

Silica functionalized sulfonic acid coated with ionic liquid has been prepared and characterized. Initially, activated silica and 3-mercaptopropyl (trimethoxy)silane were refluxed in toluene followed by oxidation of the resultant 3-mercaptopropylsilica. The silica functionalized sulfonic acid was then coated with ionic liquid [BMIM][PF_6]. The as-prepared catalyst (Silica-SO_3H-[BMIM][PF_6]) has been used for the solvent free synthesis of 1,4-dihydropyridines (Scheme I.C.9). The recyclability of the catalyst has been performed for seven cycles.[33]

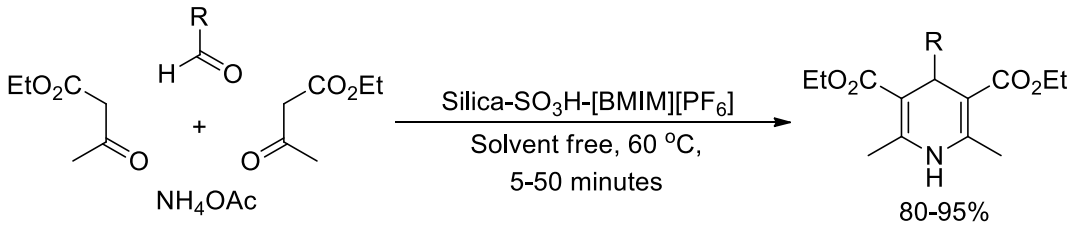

Scheme I.C.9 Silica-SO_3H-[BMIM][PF_6] catalyzed one-pot synthesis of 1,4-DHPs.

The synthesis of 1,4-dihydropyridines and N-substituted-1,4-dihydropyridines has been accomplished by using silica supported 12-tungstophosphoric acid catalyst (PW/SiO_2). The reaction conditions involve three-component condensation between aldehydes, β-ketoesters and ammonium acetate (or amines). The desired products were obtained in 55-98% at room temperature under solvent free conditions (Scheme I.C.10).[50]

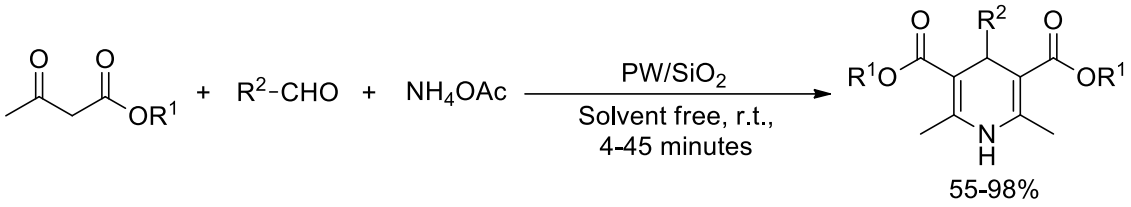

Scheme I.C.10 PW/SiO_2 catalyzed three-component synthesis of 1,4-DHPs.

Organocatalysts have been frequently used in the multicomponent synthesis of diverse heterocyclic compounds. Ultrasound assisted, *p*-TSA (*p*-toluenesulfonic acid) catalyzed synthesis of 1,4-DHPs has been achieved under aqueous micellar medium. The investigators have employed aqueous sodium dodecyl sulfate (SDS) in presence of *p*-TSA for the reaction and the corresponding products have been obtained in 90-97% yield (Scheme I.C.11). Moreover, the protocol has been further extended towards the synthesis of polyhydroquinolines.[39]

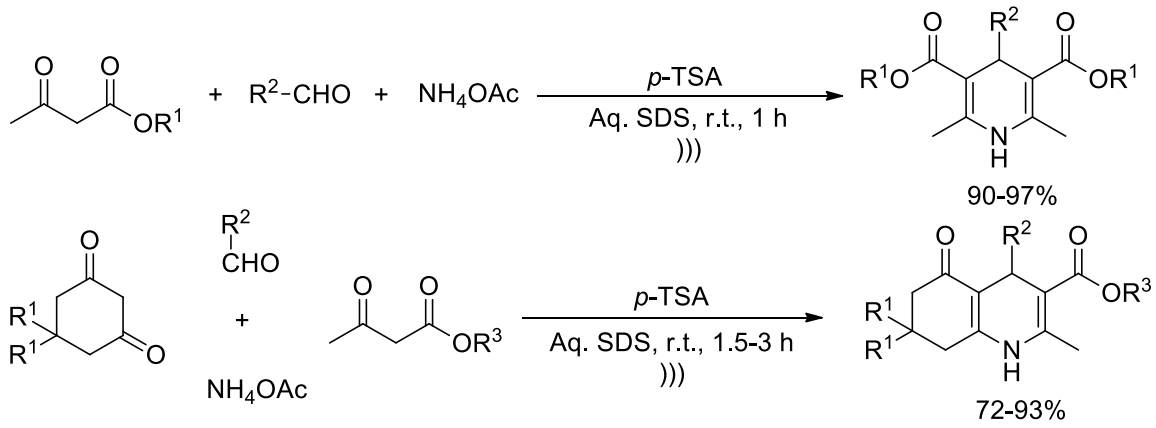

Scheme I.C.11 Ultrasound assisted synthesis of 1,4-DHPs and polyhydroquinolines in aqueous micelles.

I.C.3 Present work: Results and discussions

Graphene oxide (GO) catalyzed Hantzsch synthesis has been previously studied and reported.[51,52] However, these protocols resulted in the formation of both 1,4-dihydropyridines as well as its oxidized form, i.e. pyridine derivatives in different ratios. Moreover, the processes required elevated temperature (refluxing conditions) and no detailed recycling experiment has been performed. We supposed that GO being oxidising in nature, when used in excess, could lead to further oxidation of 1,4-DHPs to the corresponding pyridine derivatives. We therefore thought further functionalization of GO could prevent it from getting reduced and selectively form 1,4-DHP as the exclusive product. Amine functionalized graphene oxide nanosheets (AFGONs) was previously prepared, designated as NH_2–GO,[53] or

AP–GO (GO-supported primary amine),[54] and used as catalyst in Knoevenagel reaction and Henry-Michael reaction respectively. We have prepared AFGONs in our laboratory from GO and used it as an excellent bifunctional catalyst for the facile one-pot selective synthesis of dihydropyridines (DHPs), polyhydroacridines (PHAs) and polyhydroquinolines (PHQs) under ambient conditions (Scheme I.C.12). Moreover, we did not observe the formation of any oxidised pyridine derivative during the course of the reaction. We presumed that the high and selective catalytic activity of AFGONs might be due to the unique cooperative effect between amines on the basal plane of GO and the adjacent carboxylic acid functionalities on its edges.

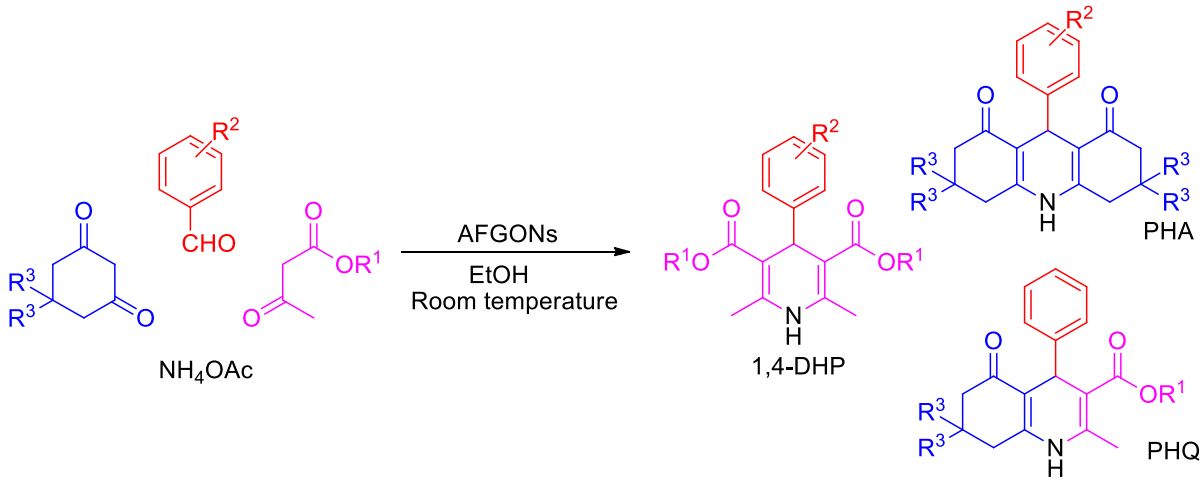

Scheme I.C.12 AFGONs catalyzed synthesis of 1,4-DHPs, PHAs and PHQs.

I.C.3.1 Preparation of the catalyst

The amine functionalized graphene oxide nanosheets (AFGONs) were prepared by following a reported procedure.[54] At first, graphene oxide was prepared by Tour's method.[55] It was then exfoliated in an ultrasonic bath for 2 h and then the amine groups were grafted onto the basal surface of GO through a facile amine-coupling reaction using (3-aminopropyl)triethoxysilane (Scheme I.C.13).

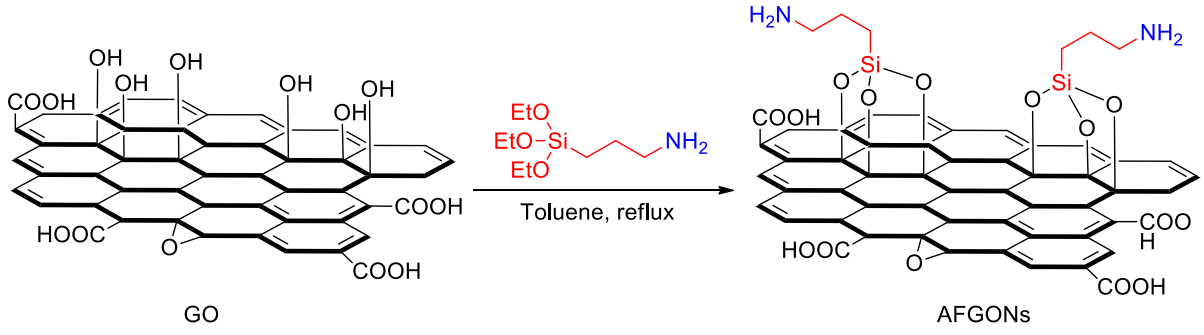

Scheme I.C.13 Illustration for the preparation of AFGONs.

I.C.3.2 Characterization of AFGONs

After the preparation of the catalyst it was characterized by FT-IR, Raman spectra, powder X-ray diffraction (XRD) and scanning electron microscopy (SEM). The FT-IR spectra of both GO and AFGONs were recorded in the range 4000-500 cm^{-1} (Figure I.C.2). The characterized bands in case of pristine GO at 3411, 1734 and 1628 cm^{-1} were due to the stretching vibrations of O–H, C=O and C=C bonds respectively.[55] The peaks in the range 1400-1000 cm^{-1} were due to the presence of C–O functionalities in GO.[55] In case of AFGONs the peaks at 2963 and 2924 cm^{-1} were due to the asymmetric and symmetric stretching modes of C–H bonds of aminopropyl groups.[53,56] The additional peak at 1593 cm^{-1} was due to the NH_2 scissor vibration, confirming the presence of terminal NH_2 in the material.[56] The band at 1123 cm^{-1} indicated Si–O–Si stretching, while the less intense band at 1198 cm^{-1} might be due to the rocking mode of SiO–C.[56] Moreover, the disappearance of the typical carbonyl band at 1734 cm^{-1} further confirmed that the carbonyl groups were converted to Si–O–C band, along with removal of oxygenated functional groups to form partially reduced graphene oxide (rGO).[57]

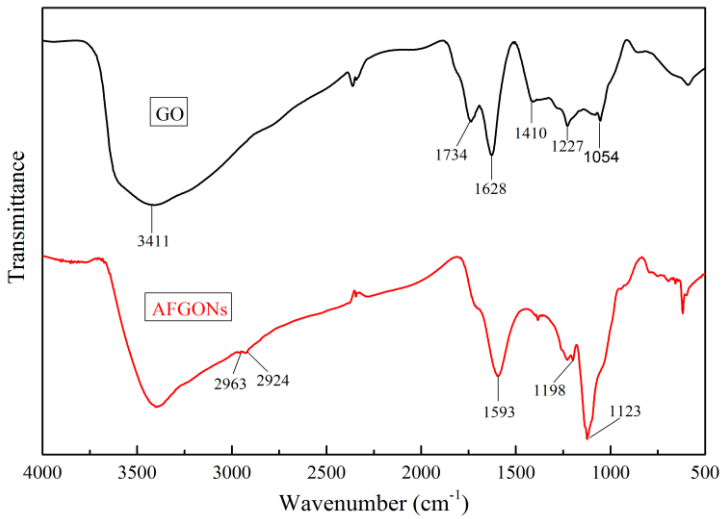

Figure I.C.2 FT-IR spectra of GO and AFGONs.

The Raman spectra of both GO and AFGONs showed characteristic D- (arising from A_{1g} vibrations of sp^2 carbon rings) and G- (arising from first order scattering of E_{2g} mode of sp^2 C atoms) bands at 1345 and 1592 cm^{-1} respectively (Figure I.C.3).[58] The intensity ratios of D- and G-bands (I_D/I_G) of GO and AFGONs were found to be 0.83 and 0.92 respectively. The higher intensity ratio (I_D/I_G) of AFGONs might indicate restoration of C=C bonds during the grafting process resulting in partial formation of rGO.[59,60]

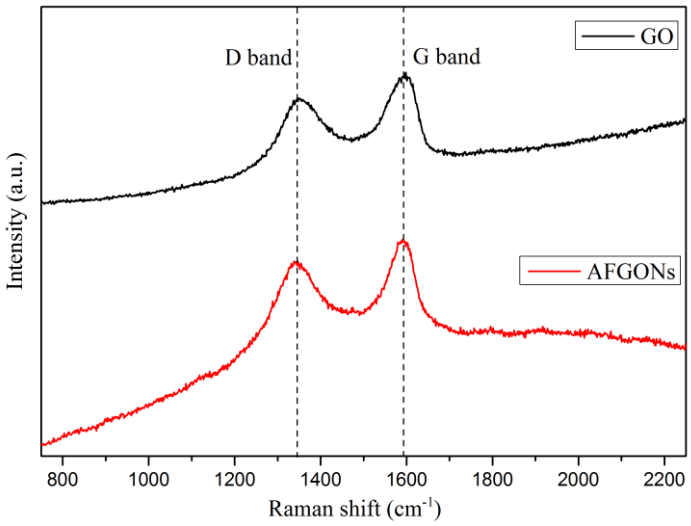

Figure I.C.3 Raman spectra of GO and AFGONs.

The X-ray diffraction (XRD) patterns of pristine GO showed a sharp peak at 2θ = 9.5° arising from the (001) plane of GO.[53] In the case of AFGONs a broad peak at 2θ = 22.1° was due to the effect of silica and the peak of GO has been shifted to 2θ = 11.9° (Figure I.C.4).[57] According to Bragg's law, 2dsinθ = nλ (λ = 0.154 nm), the interlayer distance (d) of AFGONs was found to be 7.4 Å (2θ = 11.9°) and that of GO was 9.2 Å (2θ = 9.5°) which could be attributed to the surface occupancy of aminopropyl-silica groups.[57] The characteristic peak of silica as well as the decrease in the d-spacing in case of AFGONs indicated that amino groups were fabricated on the surface of GO.[57]

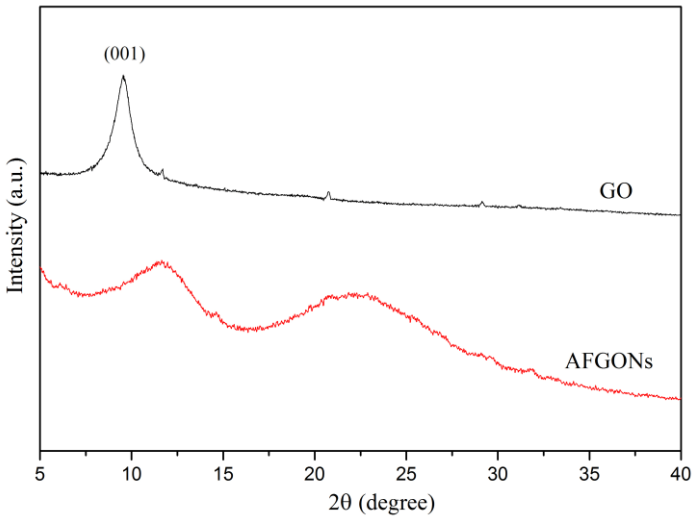

Figure I.C.4 X-ray diffraction patterns of GO and AFGONs.

The morphology of GO and AFGONs were analyzed by scanning electron microscopy (SEM). The SEM images along with the XRD patterns clearly indicated the amorphous and

fibrous nature of the catalyst (Figure I.C.5). Furthermore, the elemental composition of the AFGONs as determined by electron-dispersive X-ray spectroscopy (EDS), showed C (71.26 wt %), O (21.07 wt %), Si (3.96 wt %) and N (3.71 wt %), which confirmed the deposition of silica groups on the surface of GO (Figure I.C.6).

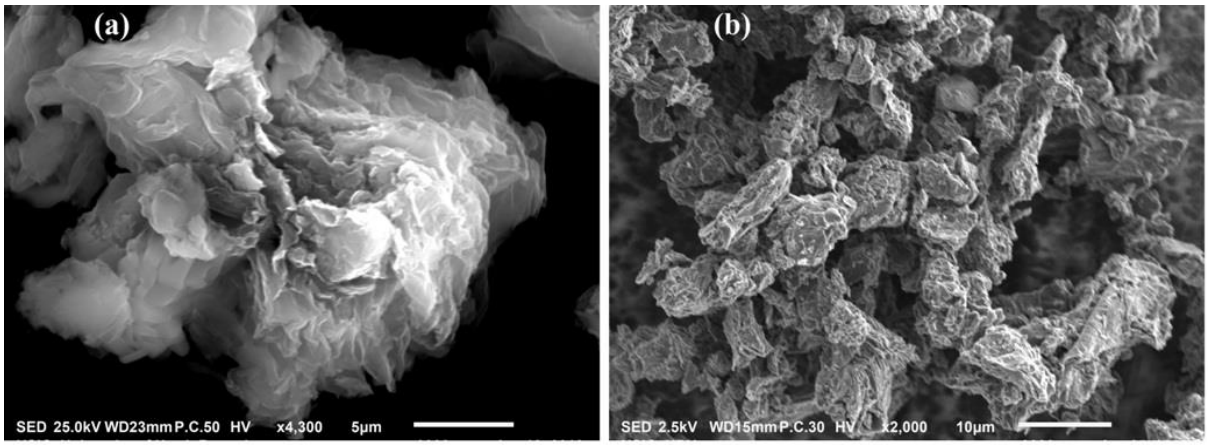

Figure I.C.5 SEM images of (a) GO and (b) AFGONs.

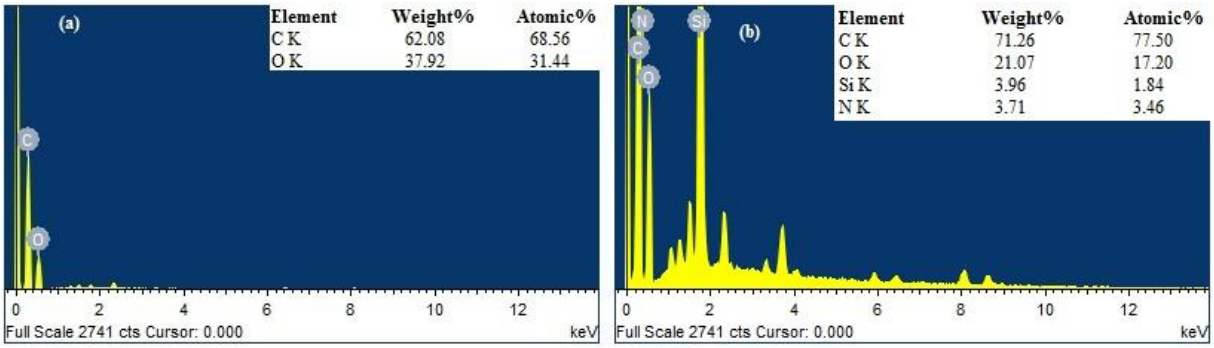

Figure I.C.6 EDS images of (a) GO and (b) AFGONs.

I.C.3.3 Catalytic activity of AFGONs: Optimization of reaction conditions

In order to optimize the reaction conditions, we began our investigation using ethyl acetoacetate (**1a**), 4-chlorobenzaldehyde (**2a**) and ammonium acetate as model substrates in the presence of AFGONs as catalyst. Initially, the reactants were screened with regard to different solvents and then the other parameters like temperature, catalyst loading and duration of reaction were varied (Table I.C.1). At first, we performed the reaction using AFGONs (50 mg) in ethanol at 78 °C. The desired product **4a** was obtained in 69% yield (entry 1). The formation of **4a** was confirmed by ^{1}H, ^{13}C NMR spectroscopy and HRMS analysis. The ^{1}H NMR peaks appearing as singlet at δ 2.33, 4.98 and 6.03 ppm were respectively due to the CH_3 groups, quaternary H and NH moieties of 1,4-DHP nucleus. Moreover, the compound **4a** was subjected to ESI-HRMS analysis and the (*m/z*) for

$C_{19}H_{22}ClNO_4$ $[M + H]^+$ was calculated at 364.1315 and found at 364.1299, which confirmed the formation of **4a**. To check the role of solvent, the reaction was carried out in various solvents like CH_3CN, H_2O and DMF (entries 2–5). The best result in terms of product yield was obtained using ethanol as solvent. Reducing the catalyst loading (25 mg) and carrying out the reaction at 50 °C increased the product yield to 72% (entry 6). Encouraged by the outcome, we carried out a reaction at room temperature (r.t.) which further increased the yield of the product to 88% (entry 7). The yield of the product was relatively lower at higher temperature as compared to room temperature. This could be due to some side reactions taking place at higher temperature as was observed on TLC. A neat mixture of the reactants without any solvent afforded the product in 52% yield (entry 8). The reaction when conducted without any catalyst resulted in poor conversion even after prolonged reaction time which indicated the imperative role of the catalyst (entry 9, 21%).

Table I.C.1 Optimization of reaction conditions[a]

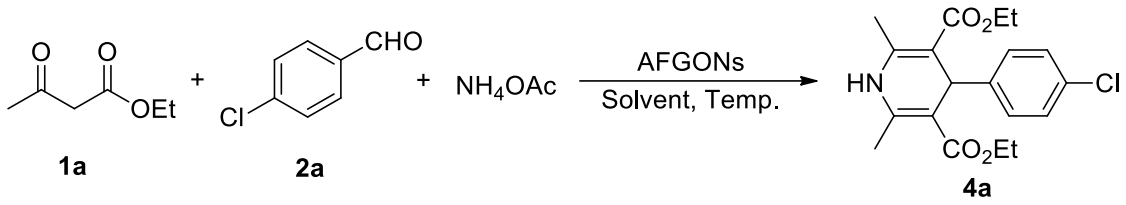

Entry	AFGONs (mg)	Solvent	Temp (°C) / time (h)	Yield (%)[b]
1	50	EtOH	78 / 8	69
2	50	CH_3CN	80 / 8	58
3	50	H_2O	90 / 8	42
4	50	H_2O	90 / 8	65[c]
5	50	DMF	80 / 8	68
6	25	EtOH	50 / 4	72
7	**25**	**EtOH**	**r.t. / 2**	**88**
8	25	–	r.t. / 2	52
9	–	EtOH	r.t. / 20	21

[a]Reaction conditions: **1a** (2 mmol), **2a** (1 mmol), NH_4OAc (2 mmol) and solvent (4 mL). [b]Isolated yield. [c]TBAB (10 mol%) was used.

I.C.3.4 Synthesis of 1,4-dihydropyridine derivatives

After the optimization of the reaction conditions, diverse 1,4-DHPs were synthesized and the results are presented in Table I.C.2. A series of different aldehydes reacted under the standard reaction conditions and in all cases the desired products were obtained in good to excellent

yields. Aromatic aldehydes substituted with both electron donating (–Cl, –Br, –CH_3, –OCH_3, –OH and –NMe_2) as well as electron withdrawing (–F and –NO_2) groups reacted efficiently to afford the corresponding products (**4a**-**k**). The substitution pattern on the aromatic moiety did not have any significant influence in the course of the reaction. We then checked the reaction with 2-naphthaldehyde and cinnamaldehyde, which furnished the desired products in 84% and 83% yield respectively (**4l** and **4m**). Further investigation with aliphatic aldehydes also worked efficiently affording the desired products (**4n** and **4o**). Fascinatingly, heterocyclic aldehydes like furfural and 5-bromo-2-thiophenecarboxaldehyde were found to be equally effective affording the anticipated products in 87% and 89% isolated yield respectively (**4p** and **4q**). In the ^{1}H NMR spectrum of **4c** the singlet peaks at δ 2.32, 3.64 and 4.95 ppm were respectively due to due to the CH_3 groups of 1,4-DHP nucleus, ester CH_3 groups and the quaternary H. The broad singlet peak δ 5.87 ppm was due to the NH moiety of 1,4-DHP nucleus. The four aromatic Hs appeared as two doublets at δ 7.14 (J = 8.4 Hz, 2H) and 7.32 (J = 8.4 Hz, 2H) ppm. In case of **4g**, the two terminal ester CH_3 groups appeared as triplets at δ 1.23 (J = 7.2 Hz) ppm. The peaks at δ 2.32 ppm were due to the two CH_3 groups of 1,4-DHP nucleus. The –NMe_2 group appeared as singlet at δ 2.88 ppm. The ester CH_2 groups appeared as quartet at δ 4.08 (J = 6.9 Hz) ppm. The quaternary H and the NH moiety appeared as singlet at δ 4.88 and 5.56 ppm. The four aromatic Hs appeared as two doublets at δ 6.60 (J = 78 Hz, 2H) and 7.14 (J = 8.4 Hz, 2H) ppm. In the ^{13}C NMR spectrum of **4g** the characteristic peak of –NMe_2 appeared at 38.3 ppm.

Table I.C.2 AFGONs catalyzed synthesis of 1,4-dihydropyridines[a]

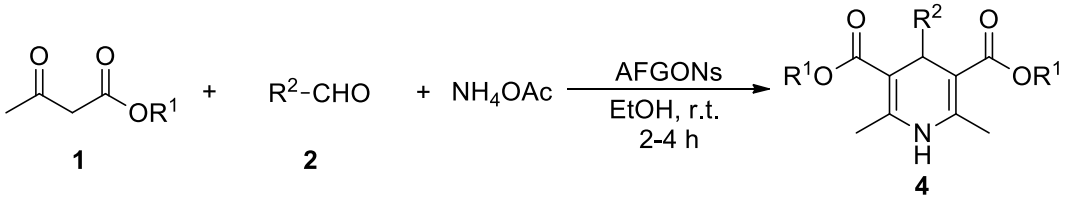

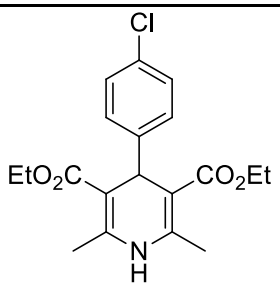	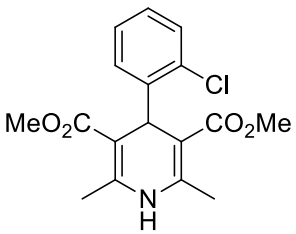	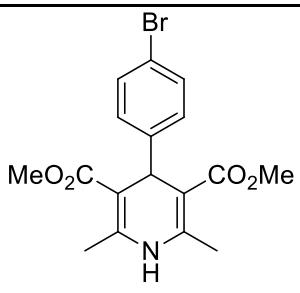
4a, 88%, 2 h	**4b**, 84%, 4 h	**4c**, 87%, 2 h

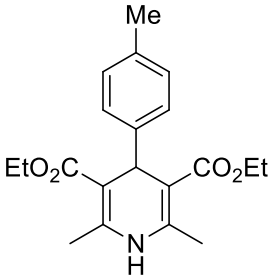

4d, 85%, 3h

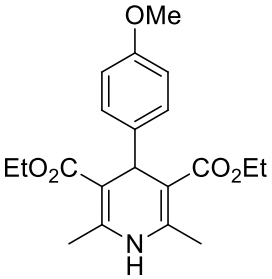

4e, 86%, 3 h

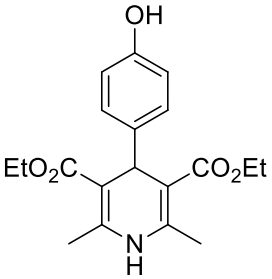

4f, 89%, 2 h

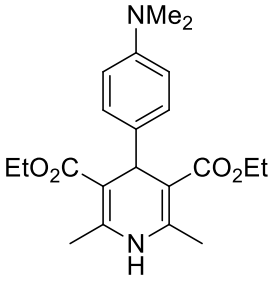

4g, 87%, 3 h

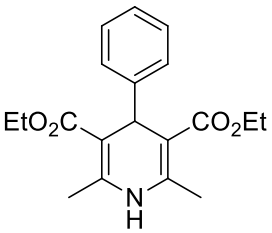

4h, 90%, 2h

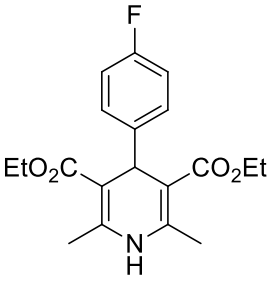

4i, 91%, 2 h

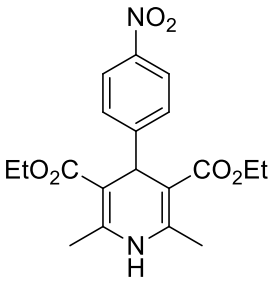

4j, 90%, 2 h

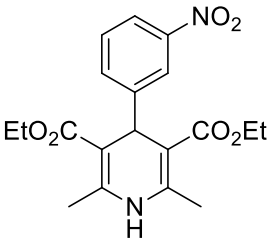

4k, 93%, 2 h

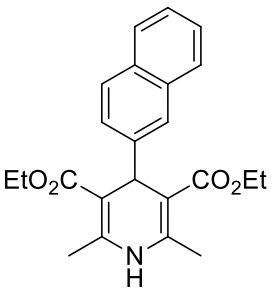

4l, 84%, 4 h

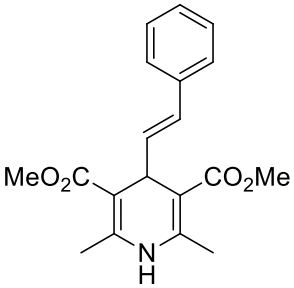

4m, 83%, 4 h

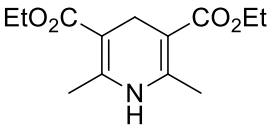

4n, 90%, 3 h

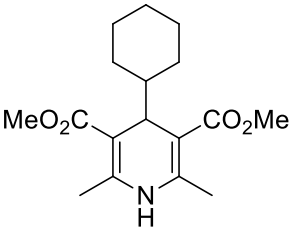

4o, 83%, 4 h

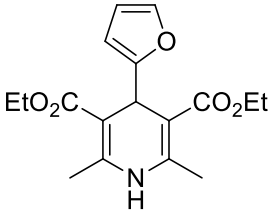

4p, 87%, 3 h

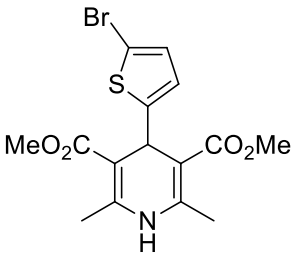

4q, 89%, 4 h

[a]Reaction conditions: **1** (2 mmol), **2** (1 mmol), NH_4OAc (2 mmol) and AFGONs (25 mg) in EtOH (4 mL) were stirred at r.t. for 2-4 h.

I.C.3.5 Synthesis of 1,8-dioxodecahydroacridine derivatives

The scope of the protocol was further extended towards the synthesis of 1,8-dioxodecahydroacridines (Table I.C.3). Acridinediones possesses potential biological and pharmacological properties. For instance 1,8-dioxodecahydroacridine derivatives exhibit a wide range of biological properties such as anti-malarial, anti-tumour, anticancer, anti-microbial activities and used as β-channel opener in case of cardiovascular diseases.[34,48] Moreover, some derivatives of acridinediones has been used in laser dyes and photo initiators because of their florescent properties.[46] The pseudo four-component reaction was accomplished with benzaldehydes bearing both electron withdrawing (–F, $–NO_2$) as well as electron donating (–Cl, –Br, –OH, –OMe) groups. The substitution pattern on the aldehyde partner did not affect the product yield. The formation of the desired products was confirmed by NMR spectroscopy. The compound **5d** showed distinct singlet peaks for the two dimedone CH_3 groups at δ 0.95 and 1.07 ppm. The quaternary H and the NH moiety appeared as singlet at δ 5.06 and 7.47 ppm respectively. The eight dimedone CH_2 hydrogen appeared as multiplet between 2.12-2.35 ppm. In the ^{13}C NMR spectrum heteronuclear coupling between ^{13}C and ^{19}F occurred and the peaks appeared at δ 32.8 (d, J = 28.5 Hz), 114.7 (d, J = 21.0 Hz) and 129.4 (d, J = 8.2 Hz) ppm.

Table I.C.3 AFGONs catalyzed synthesis of 1,8-dioxodecahydroacridine[a]

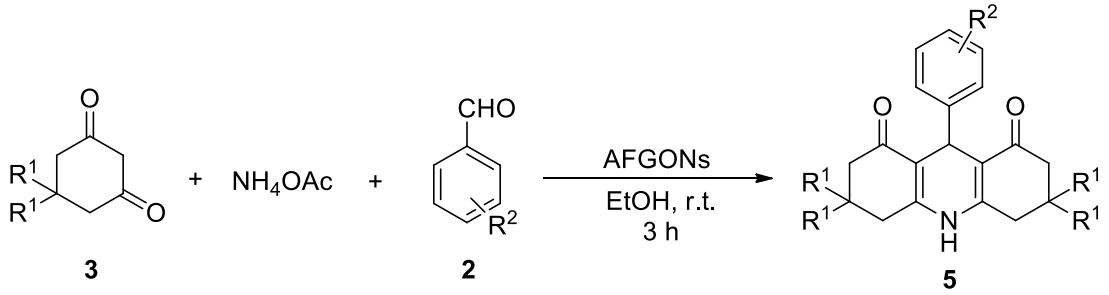

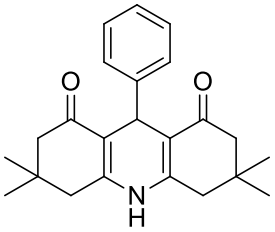	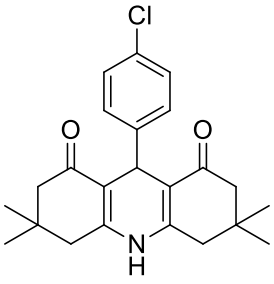	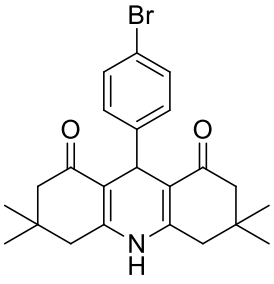
5a, 90%	**5b**, 89%	**5c**, 91%

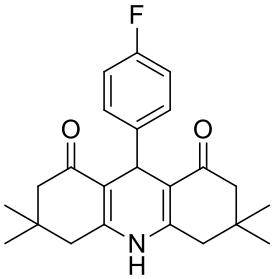

5d, 92%

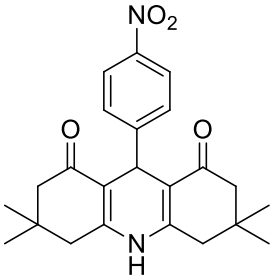

5e, 90%

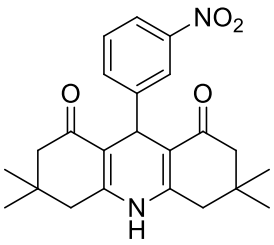

5f, 91%

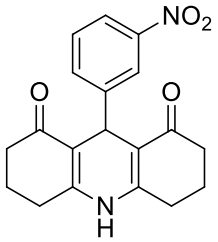

5g, 88%

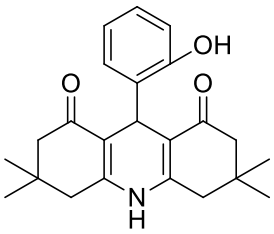

5h, 86%

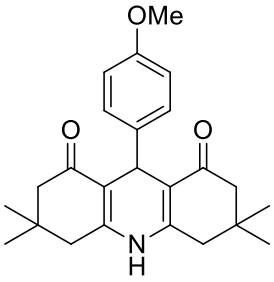

5i, 89%

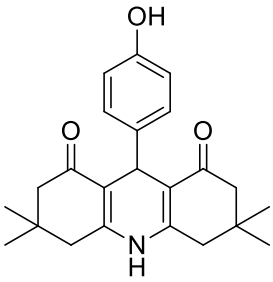

5j, 86%

[a]Reaction conditions: **3** (2 mmol), **2** (1 mmol), NH_4OAc (2 mmol), AFGONs (25 mg) and EtOH (4 mL) were stirred at r.t. for 3 h.

I.C.3.6 Synthesis of polyhydroquinoline derivatives

Polyhydroquinolines (PHQs) are unsymmetrical derivatives of 1,4-DHPs which displays prominent biological activities associated with cardiovascular diseases and hypertension.[37] Certain 2,4-disubstituted polyhydroquinoline derivatives are active glycogen phosphorylase inhibitors and exhibits anti-hyperglycemic activity.[61] We explored the synthesis of PHQs through four-component catalytic reaction between β-ketoester, aldehyde, dimedone/cyclohexan-1,3-dione and ammonium acetate. Gratifyingly, the reaction worked efficiently and the desired products were obtained in good to excellent yields (Table I.C.4). Benzaldehydes bearing both electron donating groups (–Me, $–CHMe_2$, –Br, –OH) as well as electron withdrawing groups (–F, $–NO_2$) were well tolerated in the course of the reaction. Furthermore, the four-component reaction did not result in the formation of any symmetrical 1,4-DHP derivatives. The compound **6c** was characterized by ^1H, ^{13}C spectroscopy and

HRMS analysis. The two terminal CH_3 moieties of isopropyl groups appeared as doublet at δ 1.17 (J = 6.9 Hz) ppm, and the CH hydrogen appeared as multiplet between δ 2.75-2.84 ppm. Furthermore, compound **6c** was analyzed by ESI-HRMS and the (m/z) $C_{23}H_{29}NO_3$ $[M + H]^+$ was calculated at 368.2225 and found at 368.2231, which confirmed the formation of **6c**.

Table I.C.4 AFGONs catalyzed four-component synthesis of polyhydroquinolines[a]

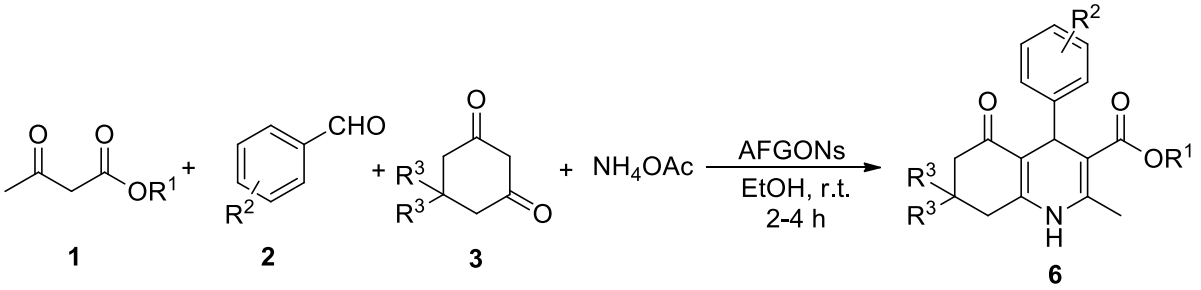

1 2 3 6

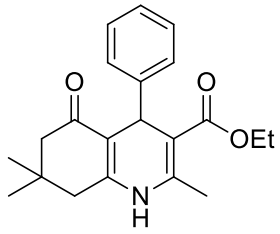

6a, 90%, 2 h

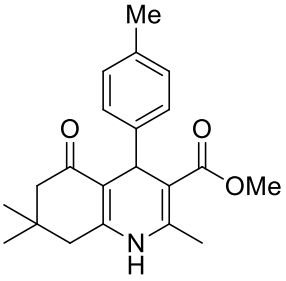

6b, 87%, 4 h

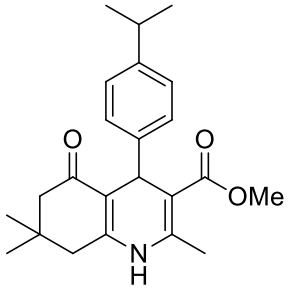

6c, 91%, 3 h

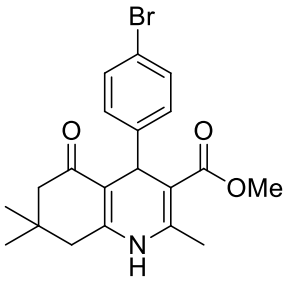

6d, 90%, 2 h

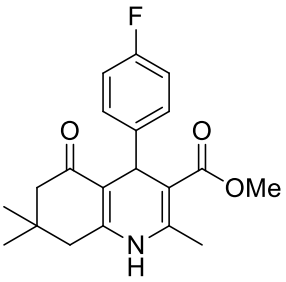

6e, 89%, 4 h

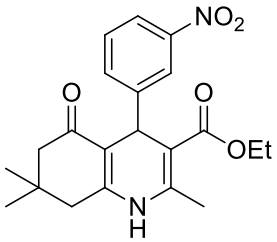

6f, 90%, 2 h

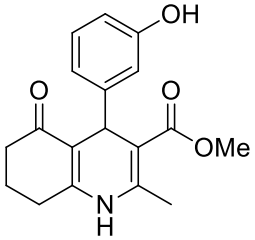

6g, 84%, 4 h

[a]Reaction conditions: **1** (1 mmol), **2** (1 mmol), **3** (1 mmol), NH_4OAc (2 mmol), AFGONs (25 mg) and EtOH (4 mL) were stirred at r.t. for 2-4 h.

I.C.3.7 Gram scale synthesis of 1,4-dihydropyridine (4a)

As an application of the newly developed methodology, we attempted a gram scale synthesis of 1,4-dihydropyridine (**4a**). For this purpose, ethyl acetoacetate (2.6 g, 20 mmol), 4-chlorobenzaldehyde (1.4 g, 10 mmol) and ammonium acetate (1.5 g, 20 mmol) were reacted under the standard reaction conditions using variable amounts of AFGONs (Table I.C.5). The desired product was formed in 84 % (3.05 g) isolated yield using 100 mg of catalyst (Scheme I.C.14). The results showed that proportionate increase of catalyst was not required for the gram scale synthesis.

Table I.C.5 Catalyst optimization in gram scale synthesis of 1,4-dihydropyridine (**4a**)

AFGONs (mg)	250	150	100	75
Isolated yield (%)	87	84	84	64

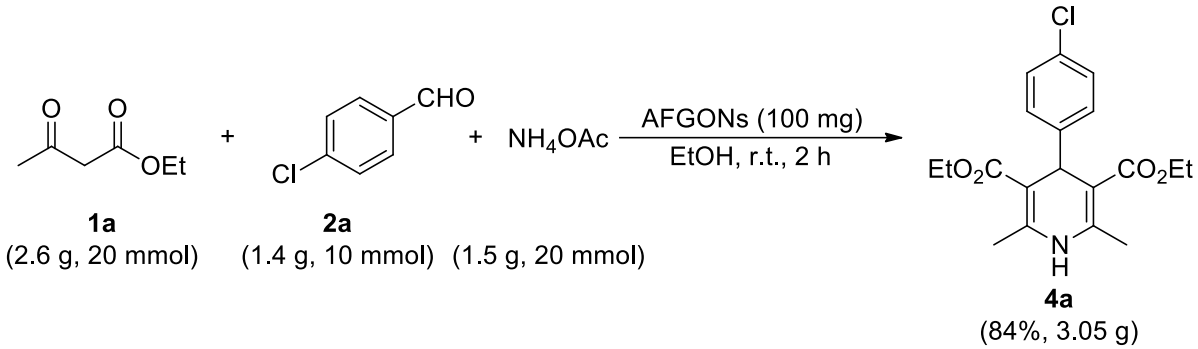

Scheme I.C.14 Gram scale synthesis of 1,4-dihydropyridine (**4a**).

I.C.3.8 Recyclability of AFGONs

We evaluated the reusability of AFGONs in the synthesis of **4a** under the optimized reaction condition. The catalyst was easily recovered from the reaction mixture by simple filtration. It was washed with ethyl acetate (3 x 5 mL) followed by water (5 mL) and was dried under vacuum for 6 h before being used for the next run. The catalyst could be used for five consecutive runs without significant loss in its catalytic activity and product yield (Figure I.C.7). Moreover, the recovered catalyst was characterized by FT-IR (Figure I.C.8 (a)), Raman spectroscopy (Figure I.C.8 (b)), X-ray powder diffraction (Figure I.C.9), SEM (Figure I.C.10) and EDS (Figure I.C.11) analysis and compared with the fresh catalyst. The results did not show any significant change in the spectral data and diffraction patterns of the catalyst before and after catalytic runs.

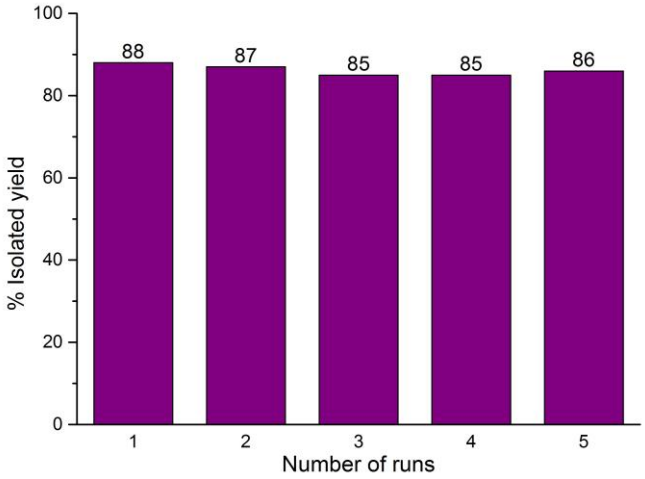

Figure I.C.7 Recyclability of AFGONs in the synthesis of 1,4-dihydropyridines.

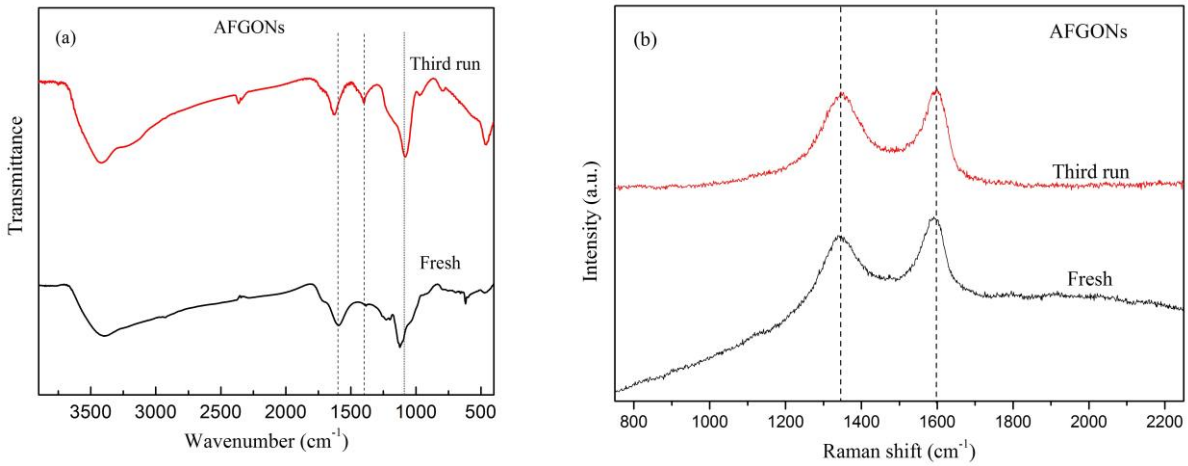

Figure I.C.8 (a) FT-IR and (b) Raman spectra of AFGONs fresh and after the third run.

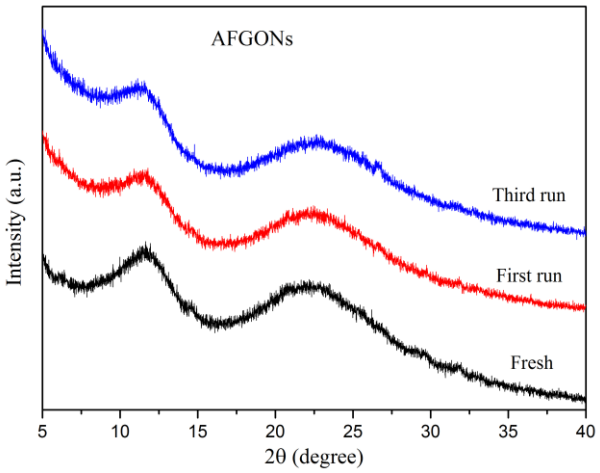

Figure I.C.9 X-ray diffraction patterns of AFGONs fresh, after first and third runs.

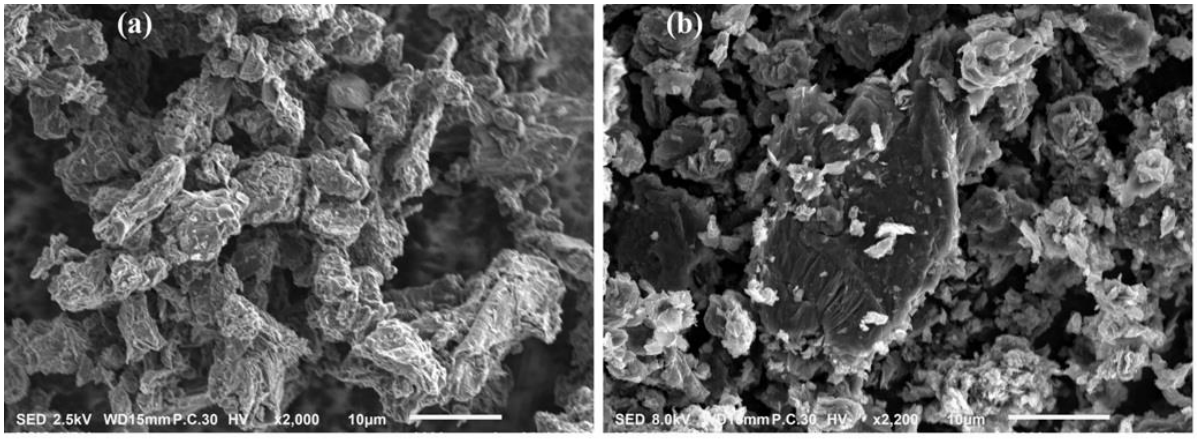

Figure I.C.10 SEM images AFGONs (a) fresh and (b) after the third run.

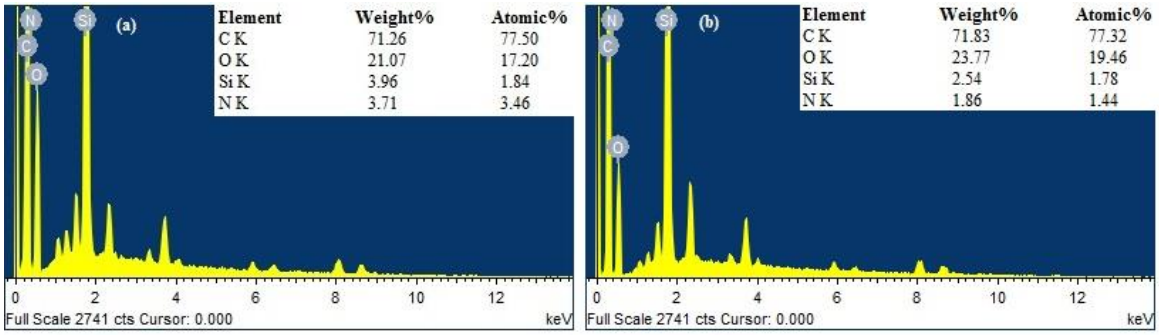

Figure I.C.11 EDS images of AFGONs (a) fresh and (b) third run.

I.C.3.9 Control experiments

The proposed mechanism for the formation of 1,4-DHP involves two key intermediates **7** and **8**, generated respectively by the aldol condensation of one equivalent of ethyl acetoacetate with aldehyde and the reaction of second equivalent of ethyl acetoacetate with ammonia.[38] We set up three control experiments under the optimized reaction conditions (Scheme I.C.14). The first reaction was performed by using ethyl acetoacetate (1 mmol) and 4-chlorobenzaldehyde (1 mmol) and the second reaction using 4-chlorobenzaldehyde (1 mmol) and NH_4OAc (2 mmol). The third reaction was carried out with ethyl acetoacetate (1 mmol) and NH_4OAc (2 mmol). The first and the second reaction did not result in the formation of any new products or intermediates even after 24 h. The HPLC analysis of the third reaction after 1 h indicated the presence of ethyl acetoacetate (31.1%) along with two new intermediates **8** and **9** (23.3% and 45.5% respectively). Although we were not able to isolate these two intermediates (**8** and **9**), it could be enamine (**8**) and bis-enamine (**9**), whose formation from 1,3-diketo ester and amine is reported in literature.[25,62,63] Furthermore, the formation of intermediate **9** was supported by HRMS data.[62] We added 4-chlorobenzaldehyde

in the third reaction after 1 h, which instantly gave the desired product (**4a**), which confirmed that the reaction proceeded through the formation of enamine intermediates. Moreover, the addition of **7** which was prepared by Knoevenagel condensation of ethyl acetoacetate and 4-chlorobenzaldehyde using piperidine,[64] to the third reaction after 1 h did not give **4a**, which further confirmed that the reaction mechanism does not involve intermediate **7**.

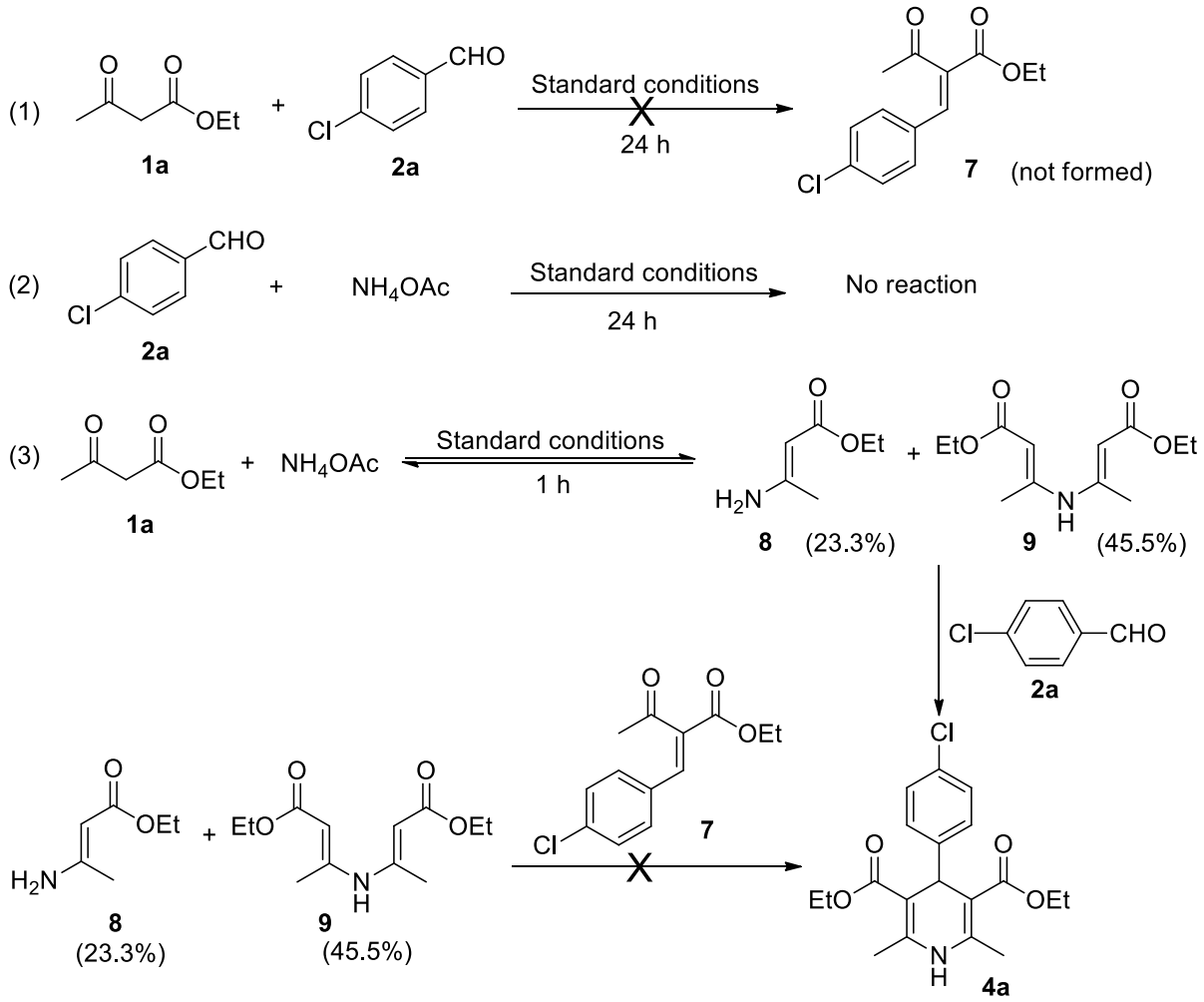

Scheme I.C.15 Control experimental analysis.

I.C.3.10 Plausible mechanism for the synthesis of 1,4-dihydropyridine

On the basis of the results obtained from control experiments, a mechanistic pathway for the 1,4-DHP synthesis was proposed (Scheme I.C.15). The acidic moiety present in the catalyst was involved in the activation of carbonyl groups of both ethyl acetoacetate and the aldehyde. Initially, the bis-enamine intermediate (**9**) was formed by the reaction of two equivalents of ethyl acetoacetate with ammonia generated from ammonium acetate. This was followed by the addition of aldehyde with bis-enamine (**9**) to form intermediate **10**. The basic moiety of the catalyst then abstracted a proton from **10** aiding in the cyclization to intermediate **11**

along with the elimination of one molecule of H_2O. Finally, the abstraction of another proton from **11** resulted in the formation of the desired 1,4-dihydropyridine.

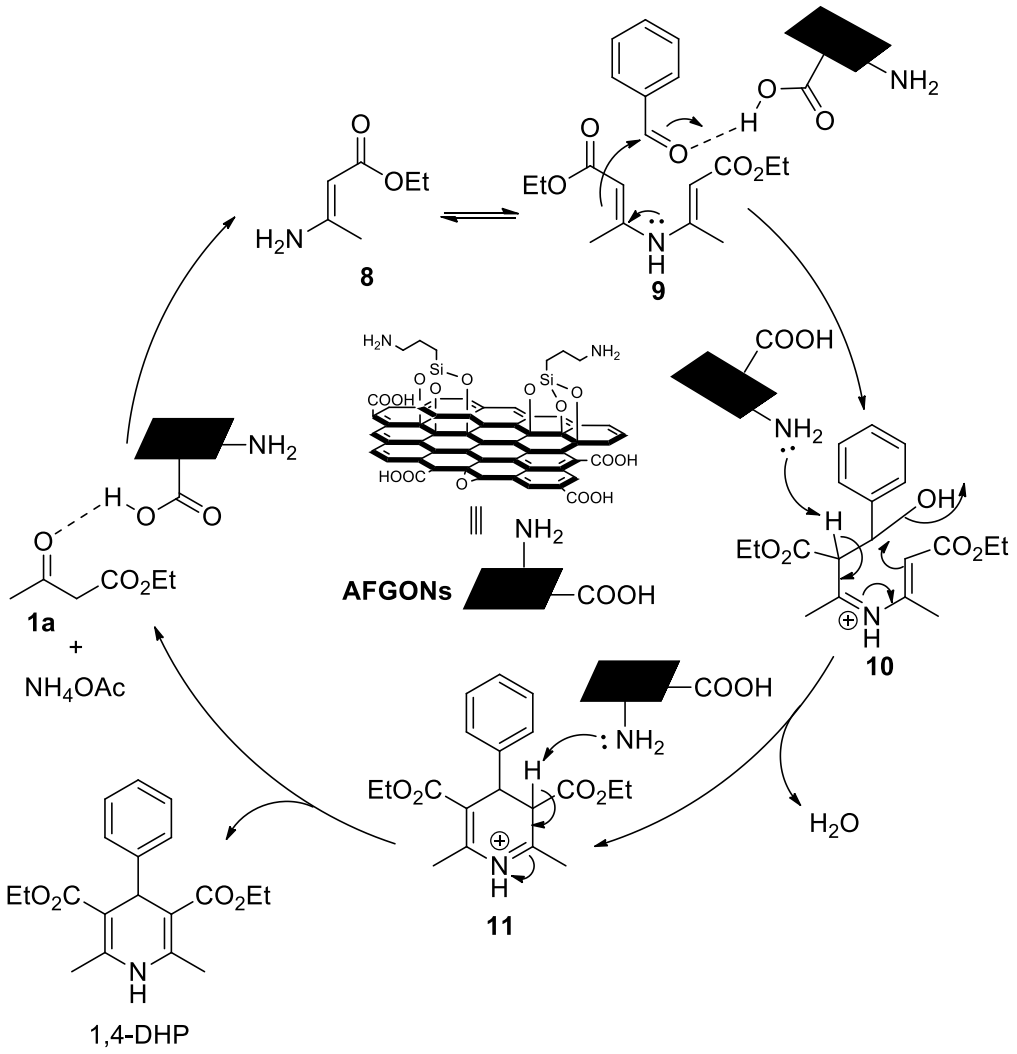

Scheme I.C.16 Plausible mechanism for the synthesis of 1,4-DHPs.

I.C.3.11 Comparison of AFGONs with previously reported catalytic systems

The efficiency of AFGONs was compared with previously reported catalytic systems for the synthesis of 1,4-DHPs (Table I.C.6). The reaction between benzaldehyde, ethyl acetoacetate and ammonium acetate was selected as the model reaction for this purpose. The results confirmed that AFGONs exhibited superior catalytic performance in terms low catalyst loading and ease of purification of products. Besides, room temperature reaction condition was an added advantage of this protocol.

Table I.C.6 Comparison of AFGONs with reported catalyst for the synthesis of 1,4-DHPs

Entry	Catalyst	Reaction conditions	Time	Yield (%)	Reference
1	$HClO_4$-SiO_2 (50 mg)	Solvent free/80 ^oC	20 min	95	65
2	ZrO_2-SO_3H (100 mg)	Solvent free/80 ^oC	12 min	94	66
3	Alginic acid (10 mol%)	EtOH/reflux	50 min	97	67
4	Cellulose sulfuric acid (50 mg)	Solvent free/80 ^oC	5 h	90	31†
5	Sulfated polyborate (5 wt%)	Solvent free/90 ^oC	15 min	95	41
6	Chitosan NPs (100 mg)	Solvent free/80 ^oC	20 min	90	68
7	PPh_3 (20 mol%)	EtOH/reflux	5 h	72	45†
8	$CeCl_3 \cdot 7H_2O$ (10 mol%)	CH_3CN/r.t.	3 h	80	69†
9	PdRuNi@GO (6 mg)	DMF/70 ^oC	45 min	88	36
10	AFGONs (25 mg)	EtOH/r.t.	2 h	90	This work

†Catalyst was not recyclable.

I.C.4 Conclusion

In conclusion, we have developed an eco-friendly route for the selective preparation of Hantzsch pyridines and related heterocyclic biomolecules via a one-pot multicomponent reaction using amine functionalized graphene oxide nanosheets (AFGONs). We have demonstrated that suitable tuning of GO prevented further oxidation of the product (1,4-DHP). Short reaction time, tolerance to wide range of functional groups, reusability of catalyst, green reaction profile and simple product purification procedure are the salient features of this protocol.

I.C.5 Experimental Section

I.C.5.1 General Information

All reagents were purchased from commercial suppliers and used as received. (3-Aminopropyl)triethoxysilane was purchased from TCI, India. The solvents were purchased from commercial suppliers and used after distillation. For TLC, Merck plates coated with silica gel 60, F_{254} were used. FT-IR spectra were recorded in FT-IR 8300 SHIMADZU spectrophotometer. The ^1H & ^{13}C NMR spectra were recorded at 300 MHz and 75 MHz respectively on Bruker AV 300 spectrometer in $CDCl_3$ and DMSO-d_6. Splitting patterns of protons were described as s (singlet), d (doublet), t (triplet), q (quartet), m (multiplet) and br (broad). Chemical shifts (δ) were reported in parts per million (ppm) relative to TMS as

internal standard. *J* values (coupling constant) were reported in Hz (Hertz). ^{13}C NMR spectra were recorded with complete proton decoupling ($CDCl_3$: δ 77.0 ppm and DMSO-d_6: 39.5 ppm). Centrifugation was done in REMI R-8C DX centrifuge. The X-ray diffraction studies (PXRD) were done by the Rigaku SmartLab (9 kW) diffractometer using CuKα radiation. Raman spectra of the samples were obtained with Renishaw InVia micro Raman spectroscopy with 514 nm laser source. Scanning Electron Microscopy (SEM) and Electron Dispersive X-ray Spectroscopy (EDS) were performed using JEOL JSM-IT 100 electron microscope.

I.C.5.2 Preparation of graphene oxide (GO)

Graphene oxide was prepared by following Tour's method.[55] In this method a 9:1 (v/v) mixture of H_2SO_4 / H_3PO_4 (180:20 mL) was added to a mixture of graphite powder (1.5 g) and $KMnO_4$ (9.0 g). The mixture was then stirred at 50 °C for 12 h. After cooling the mixture to room temperature, it was gradually poured into crushed ice (200 g), which was followed by the slow addition of H_2O_2 (30%, 1.5 mL). The solution was then centrifuged (5000 rpm) and the supernatant was discarded. The residual solid material was successively washed with deionised water (100 mL) and then with 30% HCl (100 mL). The solid material was then repeatedly washed with water and centrifuged. Finally, the solid brown material was collected and dried at 60 °C under vacuum to obtain solid graphene oxide.

I.C.5.3 Preparation of AFGONs

AFGONs were prepared by following literature reported method.[54] GO (500 mg) was dispersed in anhydrous toluene (20 mL) and ultrasonically treated for 2 h. After that, (3-aminopropyl)triethoxysilane (0.85 mmol) was added to it and stirred under reflux condition for 12 h. The solvent was evaporated in a vacuum rotary evaporator and the solid powder was washed with dichloromethane and vacuum dried at 60 °C for 12 h.

I.C.5.4 General procedure for the synthesis of 1,4-dihydropyridines (4a-q) using AFGONs

A 25 mL round bottomed flask was charged with β-ketoester (2mmol), aldehyde (1mmol), ammonium acetate (2 mmol) and ethanol (4 mL). This was followed by the addition of AFGONs (25 mg). The reaction mixture was stirred at room temperature until consumption of the reactants (2-4 h) monitored by TLC. After completion of the reaction the solvent was removed under vacuum. The reaction mixture was partitioned between ethyl acetate and water and the catalyst was separated by simple filtration. The combined organic layer was dried over anhydrous sodium sulfate and concentrated under vacuum. The residue obtained was recrystallized using either methanol or ethyl acetate to afford the solid products (**4a-q**).

I.C.5.5 General procedure for the synthesis of 1,8-dioxodecahydroacridines (5a-j) using AFGONs

The same methodology for the synthesis of 1,4-DHPs was followed here replacing β-ketoester with 1,3-diketone (2 mmol).

I.C.5.6 General procedure for the synthesis of polyhydroquinolines (6a-g) using AFGONs

In a 25 mL round bottomed flask, β-ketoester (1 mmol), 1,3-diketone (1 mmol), aldehyde (1 mmol), ammonium acetate (2 mmol) and ethanol (4 mL) were added. This was followed by the addition of the AFGONs (25 mg). The reaction mixture was stirred at room temperature for 2-4 h. After completion of the reaction, monitored by TLC, the solvent was removed under vacuum. The reaction mixture was partitioned between ethyl acetate and water and the catalyst was filtered off. The combined organic layer was dried over anhydrous sodium sulfate and concentrated under vacuum. The residue obtained was recrystallized using a mixture of ethyl acetate and petroleum ether to afford the desired solid products **(6a-g)**.

I.C.5.7 Characterization data of compounds listed in Table I.C.2-I.C.4

Diethyl 4-(4-chlorophenyl)-2,6-dimethyl-1,4-dihydropyridine-3,5-dicarboxylate (4a)[67]

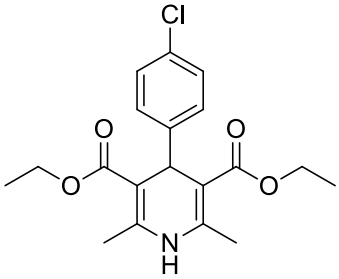

Yellow solid; m.p.: 144–146 °C (Lit. m.p.: 144–145 °C); **^{1}H NMR (300 MHz, $CDCl_3$)**: δ 1.22–1.27 (m, 6H), 2.33 (s, 6H), 4.06–4.18 (m, 4H), 4.98 (s, 1H), 6.03 (s, br, 1H), 7.18–7.30 (m, 4H); **^{13}C NMR (75 MHz, $CDCl_3$)**: δ 14.6, 19.8, 39.5, 60.2, 104.0, 128.2, 129.7, 132.0, 144.6, 146.7, 167.9; HRMS–ESI (*m/z*) calcd for $C_{19}H_{22}ClNO_4$ $[M + H]^+$ 364.1315 found 364.1299.

Dimethyl 4-(2-chlorophenyl)-2,6-dimethyl-1,4-dihydropyridine-3,5-dicarboxylate (4b)[67]

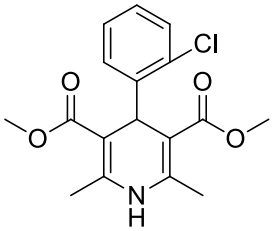

Yellow solid; m.p.: 185–186 °C (Lit. m.p.: 184–185 °C); **^{1}H NMR (300 MHz, $CDCl_3$)**: δ 2.13 (s, 3H), 2.50 (s, 3H), 3.62 (s, 3H), 3.70 (s, 3H), 5.75 (s, br, 1H), 5.96 (s, 1H), 7.20–7.26

(m, 3H), 7.36–7.38 (m, 1H); **^{13}C NMR (75 MHz, $CDCl_3$)**: δ 19.4, 21.3, 50.7, 51.2, 51.5, 103.6, 107.3, 127.1, 129.3, 129.7, 132.3, 137.6, 149.1, 154.6, 166.6, 168.0.

Dimethyl 4-(4-bromophenyl)-2,6-dimethyl-1,4-dihydropyridine-3,5-dicarboxylate (4c)[67]

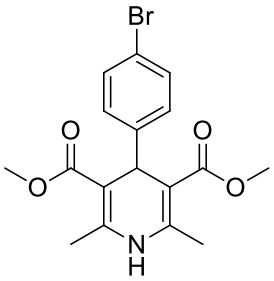

Yellow solid; m.p.: 199–200 °C (Lit. m.p.: 201–202 °C); **^{1}H NMR (300 MHz, $CDCl_3$)**: δ 2.32 (s, 6H), 3.64 (s, 6H), 4.95 (s, 1H), 5.87 (s, br, 1H), 7.14 (d, *J* = 8.4 Hz, 2H), 7.32 (d, *J* = 8.4 Hz, 2H); **^{13}C NMR (75 MHz, $CDCl_3$)**: δ 19.6, 39.0, 51.1, 103.4, 120.0, 129.5, 131.1, 144.5, 146.5, 167.8.

Diethyl 2,6-dimethyl-4-(*p*-tolyl)-1,4-dihydropyridine-3,5-dicarboxylate (4d)[67]

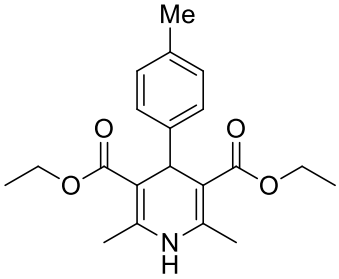

Yellow solid; m.p.: 135–136 °C (Lit. m.p.: 135–137 °C); **^{1}H NMR (300 MHz, $CDCl_3$)**: δ 1.22 (t, *J* = 6.9 Hz, 6H), 2.27–2.34 (m, 9H), 4.04–4.11 (m, 4H), 4.94 (s, 1H), 5.78 (s, br, 1H), 7.01 (d, *J* = 7.8 Hz, 2H), 7.16 (d, *J* = 7.8 Hz, 2H); **^{13}C NMR (75 MHz, $CDCl_3$)**: δ 14.2, 19.5, 21.0, 39.0, 59.6, 104.1, 127.7, 128.0, 128.5, 135.4, 143.8, 144.8, 167.6.

Diethyl 4-(4-methoxyphenyl)-2,6-dimethyl-1,4-dihydropyridine-3,5-dicarboxylate (4e)[67]

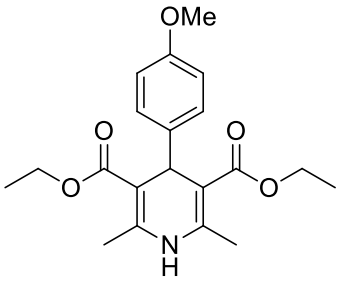

Yellow solid; m.p.: 160–161 °C (Lit. m.p.: 160–161 °C); **^{1}H NMR (300 MHz, $CDCl_3$)**: δ 1.20–1.28 (m, 6H), 2.31–2.34 (m, 6H), 3.76 (s, 3H), 4.06–4.17 (m, 4H), 4.96 (s, 1H), 5.85 (s, br, 1H), 6.78 (d, *J* = 8.7 Hz, 2H), 7.22 (d, *J* = 8.7 Hz, 2H); **^{13}C NMR (75 MHz, $CDCl_3$)**: δ 14.5, 19.8, 39.0, 55.4, 60.0, 104.5, 113.4, 129.2, 140.6, 144.0, 158.1, 168.0.

Diethyl 4-(4-hydroxyphenyl)-2,6-dimethyl-1,4-dihydropyridine-3,5-dicarboxylate (4f)[67]

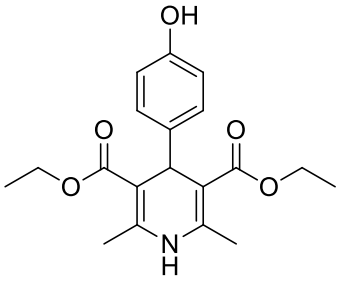

Pale yellow solid; m.p.: 229-230 °C (Lit. m.p.: 228–231 °C); **^{1}H NMR (300 MHz, DMSO–d_6)**: δ 1.12 (t, *J* = 6.6 Hz, 6H), 2.23 (s, 6H), 3.95–3.99 (m, 4H), 4.73 (s, 1H), 6.57 (d, *J* = 7.8 Hz, 2H), 6.92 (d, *J* = 7.8 Hz, 2H), 8.71 (s, br, 1H), 9.09 (s, br, 1H); **^{13}C NMR (75 MHz, DMSO–d_6)**: δ 14.1, 18.1, 37.8, 58.8, 102.2, 114.4, 128.2, 138.8, 144.6, 155.3, 167.0.

Diethyl 4-(4-dimethylaminophenyl)-2,6-dimethyl-1,4-dihydropyridine-3,5-dicarboxylate (4g)[70]

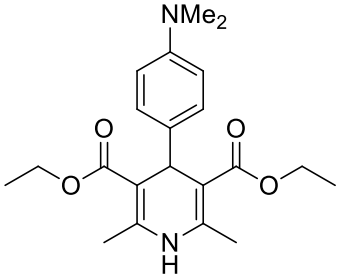

Pale yellow solid; m.p.: 158–161 °C (Lit. m.p.:158–162 °C); **^{1}H NMR (300 MHz, $CDCl_3$)**: δ 1.23 (t, *J* = 7.2 Hz, 6H), 2.32 (s, 6H), 2.88 (s, 6H), 4.08 (q, *J* = 6.9 Hz, 4H), 4.88 (s, 1H), 5.56 (s, 1H), 6.60 (d, *J* = 7.8 Hz, 2H), 7.14 (d, *J* = 8.4 Hz, 2H); **^{13}C NMR (75 MHz, $CDCl_3$)**: δ 14.3, 19.6, 38.3, 40.7, 59.6, 104.5, 112.3, 128.5, 136.4, 143.3, 149.1, 167.8.

Diethyl 2,6-dimethyl-4-phenyl-1,4-dihydropyridine-3,5-dicarboxylate (4h)[67]

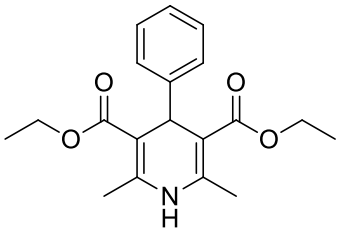

Yellow solid; m.p.: 156–158 °C (Lit. m.p.: 156–158 °C); **^{1}H NMR (300 MHz, $CDCl_3$)**: δ 1.21 (t, *J* = 7.2 Hz, 6H), 2.31 (s, 6H), 4.04–4.13 (m, 4H), 4.98 (s, 1H), 5.91 (s, br, 1H), 7.11–7.29 (m, 5H); **^{13}C NMR (75 MHz, $CDCl_3$)**: δ 14.6, 19.8, 39.9, 60.1, 104.3, 126.4, 128.1, 128.3, 144.4, 148.1, 168.1.

Diethyl 4-(4-fluorophenyl)-2,6-dimethyl-1,4-dihydropyridine-3,5-dicarboxylate (4i)[67]

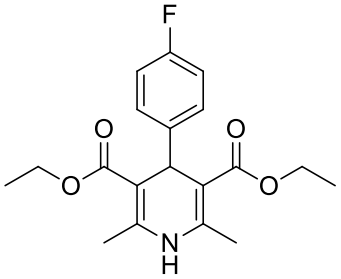

Yellow solid; m.p.: 152–153 °C (Lit. m.p.: 151–153 °C); **^{1}H NMR (300 MHz, $CDCl_3$)**: δ 1.21 (t, *J* = 7.2 Hz, 6H), 2.31 (s, 6H), 4.04–4.14 (m, 4H), 4.96 (s, 1H), 5.94 (s, br, 1H), 6.85–6.91 (m, 2H), 7.21–7.27 (m, 2H); **^{13}C NMR (75 MHz, $CDCl_3$)**: δ 14.1, 19.4, 38.9, 59.7, 103.9, 114.4 (d, *J* = 20.8 Hz), 129.3 (d, *J* = 7.7 Hz), 143.8 (d, *J* = 28.2 Hz), 159.6, 162.8, 167.5.

Diethyl 2,6-dimethyl-4-(4-nitrophenyl)-1,4-dihydropyridine-3,5-dicarboxylate (4j)[67]

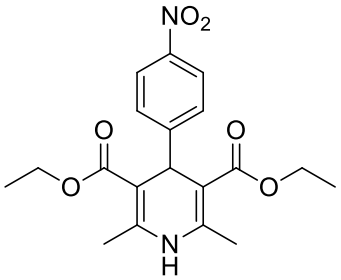

Yellow crystalline solid; m.p.: 125–126 °C (Lit. m.p.: 125–127 °C); **^{1}H NMR (300 MHz, $CDCl_3$)**: δ 1.22 (t, *J* = 6.9 Hz, 6H), 2.34 (s, 6H), 4.09 (d, *J* = 7.2 Hz, 4H), 5.01 (s, 1H), 6.16 (s, br, 1H), 7.46 (d, *J* = 8.1 Hz, 2H), 8.08 (d, *J* = 8.1 Hz, 2H); **^{13}C NMR (75 MHz, $CDCl_3$)**: δ 14.1, 19.4, 40.0, 59.9, 102.9, 123.2, 128.8, 144.8, 146.1, 155.1, 167.1.

Diethyl 2,6-dimethyl-4-(3-nitrophenyl)-1,4-dihydropyridine-3,5-dicarboxylate (4k)[67]

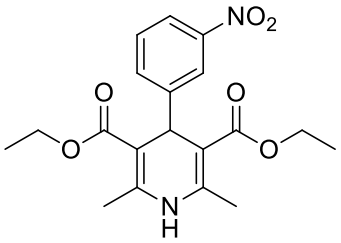

Yellow crystalline solid; m.p.: 165–166 °C (Lit. m.p.: 166–168 °C); **^{1}H NMR (300 MHz, $CDCl_3$)**: δ 1.22 (t, *J* = 7.2 Hz, 6H), 2.35 (s, 6H), 4.03–4.14 (m, 4H), 5.09 (s, 1H), 6.15 (s, br, 1H), 7.38 (t, *J* = 7.8 Hz, 1H), 7.65 (d, *J* = 7.8 Hz, 1H), 7.98–8.02 (m, 1H), 8.13 (t, *J* = 2.1 Hz, 1H); **^{13}C NMR (75 MHz, $CDCl_3$)**: δ 14.2, 19.5, 39.9, 60.0, 103.1, 121.3, 123.1, 128.6, 134.5, 145.0, 148.1, 150.0, 167.2.

Diethyl 2,6-dimethyl-4-(naphthalen-2-yl)-1,4-dihydropyridine-3,5-dicarboxylate (4l)[69]

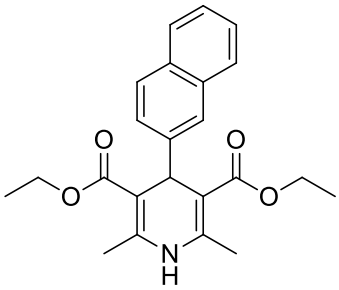

Yellow crystalline solid; m.p.: 192–193 °C (Lit. m.p.: 196 °C); **^{1}H NMR (300 MHz, $CDCl_3$)**: δ 1.21 (t, *J* = 7.2 Hz, 6H), 2.31 (s, 3H), 4.06 (q, *J* = 7.2 Hz, 4H), 5.16 (s, 1H), 6.08 (s, br, 1H), 7.36–7.49 (m, 3H), 7.66–7.75 (m, 4H); **^{13}C NMR (75 MHz, $CDCl_3$)**: δ 14.1, 19.4, 39.8, 59.7, 103.7, 125.0, 125.4, 126.1, 127.0, 127.3, 127.7, 132.1, 133.2, 144.1, 145.1, 167.7.

Dimethyl 2,6-dimethyl-4-styryl-1,4-dihydropyridine-3,5-dicarboxylate (4m)[67]

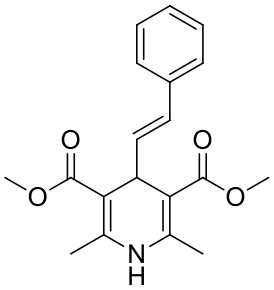

Yellow crystalline solid; m.p.: 172–174 °C (Lit. m.p.: 174–175 °C); **^{1}H NMR (300 MHz, $CDCl_3$)**: δ 2.33 (s, 6H), 3.72 (s, 6H), 4.61 (d, *J* = 4.2 Hz, 1H), 5.86 (s, br, 1H), 6.17 (d, *J* = 5.4 Hz, 2H), 7.09-7.20 (m, 1H), 7.23-7.33 (m, 4H); **^{13}C NMR (75 MHz, $CDCl_3$)**: δ 19.5, 36.1, 51.2, 101.2, 126.2, 126.9, 127.9, 128.4, 131.6, 137.6, 145.3, 168.0.

Diethyl 2,6-dimethyl-1,4-dihydropyridine-3,5-dicarboxylate (4n)[67]

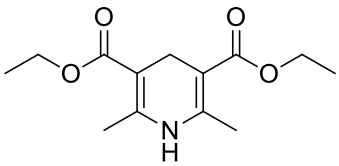

Yellow crystalline solid; m.p.: 177–179 °C (Lit. m.p.: 177–180 °C); **^{1}H NMR (300 MHz, $CDCl_3$)**: δ 1.28 (t, *J* = 8.1 Hz, 6H), 2.19 (s, 6H), 3.26 (s, 2H), 4.13–4.20 (m, 4H), 5.30 (s, br, 1H); **^{13}C NMR (75 MHz, $CDCl_3$)**: δ 14.4, 19.1, 24.7, 59.6, 99.4, 144.8, 168.0.

Dimethyl 4-cyclohexyl-2,6-dimethyl-1,4-dihydropyridine-3,5-dicarboxylate (4o)[37]

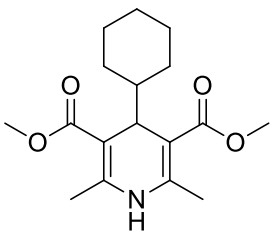

White solid; m.p.: 182–185 °C (Lit. m.p.: 184–185 °C); **^{1}H NMR (300 MHz, $CDCl_3$)**: δ 0.86–0.93 (m, 2H), 1.04–1.24 (m, 4H), 1.50–1.63 (m, 5H), 2.31 (s, 6H), 3.71 (s, 6H), 3.88 (d, *J* = 5.7 Hz, 1H), 5.93 (s, br, 1H); **^{13}C NMR (75 MHz, $CDCl_3$)**: δ 19.2, 26.5, 28.5, 38.2, 45.5, 50.8, 101.3, 144.9, 169.1.

Diethyl 4-(furan-2-yl)-2,6-dimethyl-1,4-dihydropyridine-3,5-dicarboxylate (4p)[67]

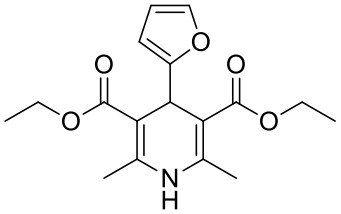

Brown solid; m.p.: 159–161 °C (Lit. m.p.: 160–161 °C); **^{1}H NMR (300 MHz, $CDCl_3$)**: δ 1.262 (t, *J* = 7.2 Hz, 6H), 2.32 (s, 6H), 4.07–4.21 (m, 4H), 5.19 (s, 1H), 5.93–6.02 (m, 2H), 6.20 (s, br, 1H), 7.20 (s, 1H); **^{13}C NMR (75 MHz, $CDCl_3$)**: δ 14.3, 19.4, 33.3, 59.8, 100.6, 104.4, 110.0, 140.8, 145.2, 158.6, 167.5.

Dimethyl 4-(5-bromothiophen-2-yl)-2,6-dimethyl-1,4-dihydropyridine-3,5-dicarboxylate (4q)[63]

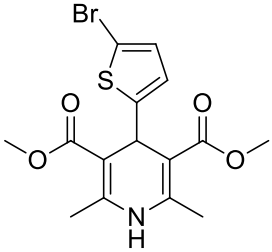

White solid; m.p.: 149–152 °C (Lit. m.p.: 150–154 °C); **^{1}H NMR (300 MHz, DMSO–d_6)**: δ 2.27 (s, 6H), 3.62 (s, 6H), 5.08 (s, 1H), 6.47 (d, *J* = 3.3 Hz, 1H), 6.93 (d, *J* = 3.6 Hz, 1H), 9.16 (s, br, 1H); **^{13}C NMR (75 MHz, DMSO–d_6)**: δ 18.5, 34.6, 51.3, 100.7, 108.9, 123.6, 130.2, 147.2, 153.8, 167.3.

3,3,6,6-Tetramethyl-9-phenyl-3,4,6,7,9,10-hexahydroacridine-1,8(2*H*,5*H*)-dione (5a)[46]

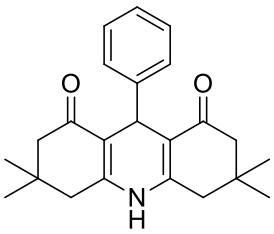

Yellow solid; m.p.: >220 °C (Lit. m.p.: 272 °C); **^{1}H NMR (300 MHz, $CDCl_3$)**: δ 0.95 (s, 6H), 1.07 (s, 6H), 2.08–2.35 (m, 8H), 5.08 (s, 1H), 7.068 (t, *J* = 6.9 Hz, 1H), 7.19 (t, *J* = 7.2 Hz, 2H), 7.33 (d, *J* = 6.9 Hz, 3H); **^{13}C NMR (75 MHz, $CDCl_3$)**: δ 27.1, 29.5, 32.6, 33.5, 40.8, 50.7, 113.4, 125.9, 127.9, 146.4, 148.4, 195.7.

9-(4-Chlorophenyl)-3,3,6,6-tetramethyl-3,4,6,7,9,10-hexahydroacridine-1,8(2*H*,5*H*)-dione (5b)[46]

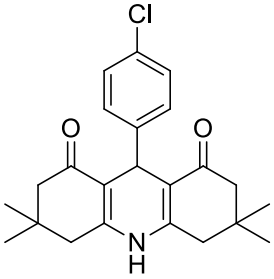

Yellow solid; m.p.: >220 °C (Lit. m.p.: 302–303 °C); **^{1}H NMR (300 MHz, $CDCl_3$)**: δ 0.93 (s, 6H), 1.05 (s, 6H), 2.03–2.28 (m, 8H), 5.05 (s, 1H), 7.15 (d, *J* = 8.4 Hz, 2H), 7.27 (d, *J* = 8.7 Hz, 2H), 8.58 (s, br, 1H); **^{13}C NMR (75 MHz, $CDCl_3$)**: δ 27.0, 29.5, 32.5, 33.3, 40.5, 50.8, 112.6, 128.0, 129.4, 131.5, 145.3, 149.8, 196.2.

9-(4-Bromophenyl)-3,3,6,6-tetramethyl-3,4,6,7,9,10-hexahydroacridine-1,8(2*H*,5*H*)-dione (5c)[46]

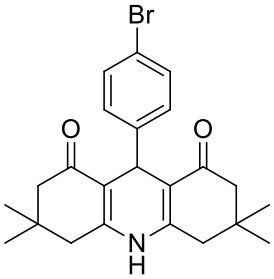

Yellow crystalline solid; m.p.: >220 °C (Lit. m.p.: >300 °C); **^{1}H NMR (300 MHz, $CDCl_3$)**: δ 0.95 (s, 6H), 1.07 (s, 6H), 2.12–2.35 (m, 8H), 5.03 (s, 1H), 7.22 (d, *J* = 8.4 Hz, 2H), 7.31 (d, *J* = 8.1 Hz, 2H), 7.43 (s, br, 1H); **^{13}C NMR (75 MHz, $CDCl_3$)**: δ 27.1, 29.5, 32.6, 33.4, 40.8, 50.7, 113.0, 119.7, 129.8, 131.0, 145.5, 148.7, 195.7.

9-(4-Fluorophenyl)-3,3,6,6-tetramethyl-3,4,6,7,9,10-hexahydroacridine-1,8(2*H*,5*H*)-dione (5d)[46]

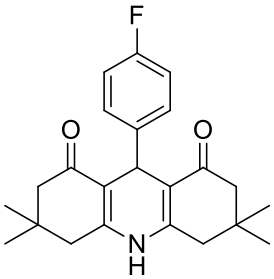

Yellow solid; m.p.: > 220 °C (Lit. m.p.: 246–248 °C); **^{1}H NMR (300 MHz, $CDCl_3$)**: δ 0.95 (s, 6H), 1.07 (s, 6H), 2.12–2.35 (m, 8H), 5.06 (s, 1H), 6.87 (t, *J* = 8.7 Hz, 2H), 7.26–7.32 (m, 2H), 7.47 (s, br, 1H); **^{13}C NMR (75 MHz, $CDCl_3$)**: δ 27.0, 29.5, 32.8 (d, *J* = 28.5 Hz), 40.8, 50.7, 113.3, 114.7 (d, *J* = 21.0 Hz), 129.4 (d, *J* = 8.2 Hz), 142.4, 148.6, 195.3.

3,3,6,6-Tetramethyl-9-(4-nitrophenyl)-3,4,6,7,9,10-hexahydroacridine-1,8(2*H*,5*H*)-dione (5e)[46]

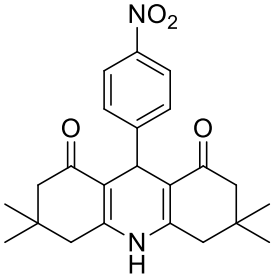

Yellow crystalline solid; m.p.: >220 °C (Lit. m.p.: 268–270 °C); **^{1}H NMR (300 MHz, $CDCl_3$)**: δ 1.12 (s, 6H), 1.24 (s, 6H), 2.30–2.52 (m, 8H), 5.54 (s, 1H), 7.25 (d, *J* = 8.4 Hz, 2H), 8.13 (d, *J* = 8.7 Hz, 2H), 11.81 (s, br, 1H); **^{13}C NMR (75 MHz, $CDCl_3$)**: δ 27.4, 29.4, 31.2, 31.4, 33.2, 46.3, 47.0, 114.8, 123.4, 127.5, 146.1, 146.5, 189.5, 190.8.

3,3,6,6-Tetramethyl-9-(3-nitrophenyl)-3,4,6,7,9,10-hexahydroacridine-1,8(2*H*,5*H*)-dione (5f)[46]

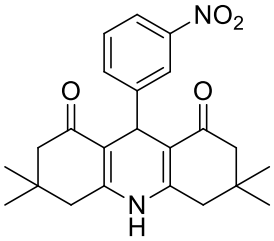

Yellow solid; m.p.: >220 °C (Lit. m.p.: 298–300 °C); **^{1}H NMR (300 MHz, $CDCl_3$)**: δ 0.97 (s, 6H), 1.10 (s, 6H), 2.13–2.45 (m, 8H), 5.17 (s, 1H), 6.41 (s, br, 1H), 7.39 (t, *J* = 7.8 Hz, 1H), 7.86–8.05 (m, 3H); **^{13}C NMR (75 MHz, $CDCl_3$)**: δ 27.1, 29.4, 32.7, 34.0, 41.2, 50.6, 112.9, 121.2, 122.2, 128.6, 135.5, 147.9, 148.1, 148.4, 195.1, 195.3; HRMS–ESI (*m/z*) calcd for $C_{23}H_{26}N_2O_4$ $[M + H]^+$ 395.1971 found 395.1978.

9-(3-Nitrophenyl)-3,4,6,7,9,10-hexahydroacridine-1,8(2*H*,5*H*)-dione (5g)[71]

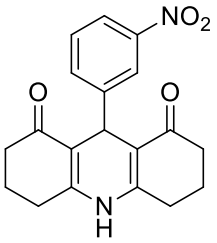

Yellow solid; m.p.: >220 °C (Lit. m.p.: 280–282 °C); **^{1}H NMR (300 MHz, DMSO–d_6)**: δ 1.04–1.90 (m, 5H), 1.95–2.19 (m, 5H), 2.23–2.43 (m, 2H), 3.86–3.95 (m, 1H), 6.95 (d, *J* = 9.6 Hz, 1H), 7.32–7.44 (m, 1H), 7.56–7.63 (m, 1H), 7.82–7.90 (m, 2H); **^{13}C NMR (75 MHz, DMSO–d_6)**: δ 20.1, 20.7, 29.1, 33.3, 37.0, 59.8, 58.9, 100.5, 101.6, 115.2, 123.5, 129.1, 147.9, 169.0, 196.1, 205.5.

9-(2-Hydroxyphenyl)-3,3,6,6-tetramethyl-3,4,6,7,9,10-hexahydroacridine-1,8(2*H*,5*H*)-dione (5h)[72]

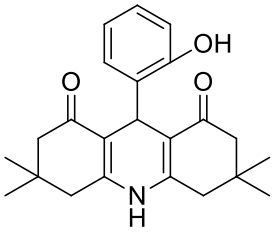

Yellow solid; m.p.: 218–219 °C (Lit. m.p.: 219–222 °C); **^{1}H NMR (300 MHz, CDCl$_3$)**: δ 0.98–1.02 (m, 8H), 1.12 (s, 3H), 1.26 (t, *J* = 7.2 Hz, 1H), (s, 3H), 2.32 (s, 3H), 2.44–2.62 (m, 2H), 4.08–4.15 (m, 1H), 4.68 (s, 1H), 7.00–7.02 (m, 3H), 7.12–7.27 (m, 1H); **^{13}C NMR (75 MHz, CDCl$_3$)**: δ 14.1, 27.1, 27.7, 29.1, 30.0, 32.2, 41.5, 49.9, 60.3, 111.0, 115.7, 118.3, 124.5, 127.4, 128.0, 151.0, 169.0, 200.7.

9-(4-Methoxyphenyl)-3,3,6,6-tetramethyl-3,4,6,7,9,10-hexahydroacridine-1,8(2*H*,5*H*)-dione (5i)[46]

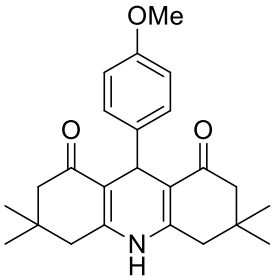

Yellow solid; m.p.: >220 °C (Lit. m.p.: >300 °C); **^{1}H NMR (300 MHz, CDCl$_3$)**: δ 1.09 (s, 5H), 1.22 (s, 7H), 2.40 (s, 8H), 3.76 (s, 3H), 5.48 (s, 1H), 6.80 (d, *J* = 7.5 Hz, 2H), 7.00 (d, *J* = 7.5 Hz), 11.91 (s, br, 1H); **^{13}C NMR (75 MHz, CDCl$_3$)**: δ 14.1, 21.0, 22.5, 27.1, 29.5, 32.5, 40.7, 50.8, 55.0, 60.3, 113.3, 128.9, 139.1, 148.7, 157.6, 171.1, 195.9.

9-(4-Hydroxyphenyl)-3,3,6,6-tetramethyl-3,4,6,7,9,10-hexahydroacridine-1,8(2*H*,5*H*)-dione (5j)[46]

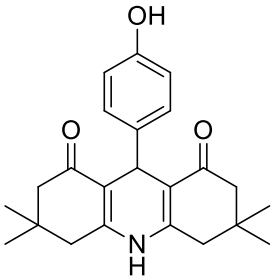

White solid; m.p.: >220 °C (Lit. m.p.: >300 °C); **^{1}H NMR (300 MHz, CDCl$_3$)**: δ 0.91 (s, 6H), 1.21 (s, 6H), 5.47 (s, 1H), 6.65 (d, *J* = 6.9 Hz, 2H), 6.90 (d, *J* = 7.2 Hz, 2H), 11.88 (s, br, 1H); **^{13}C NMR (75 MHz, CDCl$_3$)**: δ 27.3, 29.4, 31.4, 31.9, 115.2, 115.8, 127.8, 129.2, 153.9, 189.6, 190.6.

Ethyl 2,7,7-trimethyl-5-oxo-4-phenyl-1,4,5,6,7,8-hexahydroquinoline-3-carboxylate (6a)[43]

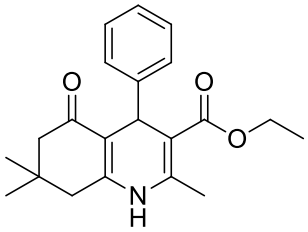

White solid; m.p.: 186–187 °C (Lit. m.p.: 186–188 °C); **^{1}H NMR (300 MHz, $CDCl_3$)**: δ 0.92 (s, 3H), 1.05 (s, 3H), 1.20 (t, *J* = 7.2 Hz, 3H), 2.15–2.25 (m, 4H), 2.31 (s, 3H), 4.06 (q, *J* = 7.2 Hz, 2H), 5.04 (s, 1H), 7.06–7.11 (m, 2H), 7.19 (t, *J* = 7.5 Hz, 2H), 7.30 (d, *J* = 7.2 Hz, 2H); **^{13}C NMR (75 MHz, $CDCl_3$)**: δ 14.2, 19.2, 27.1, 29.5, 32.6, 36.6, 40.7, 50.7, 59.8, 105.8, 111.7, 126.0, 127.8, 128.0, 144.0, 147.2, 149.3, 167.6, 195.9.

Methyl 2,7,7-trimethyl-5-oxo-4-(*p*-tolyl)-1,4,5,6,7,8-hexahydroquinoline-3-carboxylate (6b)[43]

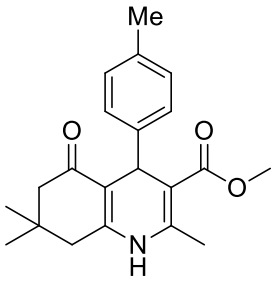

Yellow solid; m.p.: >220 °C (Lit. m.p.: 272–273 °C); **^{1}H NMR (300 MHz, $CDCl_3$)**: δ 0.94 (s, 3H), 1.07 (s, 3H), 2.18–2.23 (m, 3H), 2.25–2.31 (m, 4H), 2.37 (s, 3H), 3.61 (s, 3H), 5.02 (s, 1H), 5.84 (s, br, 1H), 7.01 (d, *J* = 7.5 Hz, 2H), 7.1 (d, *J* = 8.1 Hz, 2H); **^{13}C NMR (75 MHz, $CDCl_3$)**: δ 19.5, 21.0, 27.2, 29.4, 32.7, 35.7, 41.2, 50.7, 51.0, 105.9, 112.5, 127.6, 128.7, 135.4, 143.4, 143.8, 147.6, 167.9, 195.4.

Methyl 4-(4-isopropylphenyl)-2,7,7-trimethyl-5-oxo-1,4,5,6,7,8-hexahydroquinoline-3-carboxylate (6c)

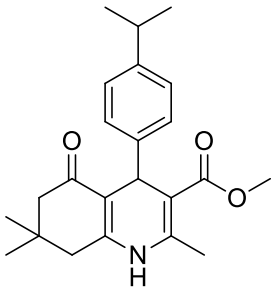

Yellow crystalline solid; m.p.: 209–213 °C; **^{1}H NMR (300 MHz, $CDCl_3$)**: δ 0.95 (s, 3H), 1.06 (s, 3H), 1.17 (d, *J* = 6.9 Hz, 6H), 2.13–2.21 (m, 2H), 2.28–2.36 (m, 5H), 2.75–2.84 (m, 1H), 3.61 (s, 3H), 5.03 (s, 1H), 7.03 (d, *J* = 8.1 Hz, 3H), 7.19 (d, *J* = 8.1 Hz, 2H); **^{13}C NMR**

(75 MHz, $CDCl_3$): δ 19.2, 23.9, 27.3, 29.4, 32.7, 33.5, 35.7, 40.8, 50.8, 51.0, 105.7, 111.8, 126.0, 127.5, 144.1, 144.3, 146.3, 149.3, 168.1, 196.0; HRMS–ESI (*m/z*) calcd for $C_{23}H_{29}NO_3$ $[M + H]^+$ 368.2225 found 368.2231.

Methyl 4-(4-bromophenyl)-2,7,7-trimethyl-5-oxo-1,4,5,6,7,8-hexahydroquinoline-3-carboxylate (6d)[43]

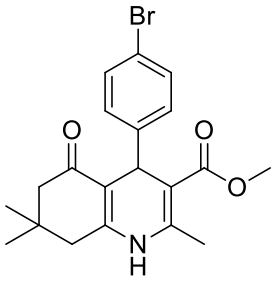

Yellow crystalline solid; m.p.: >220 °C (Lit. m.p.: 263–265 °C); **^{1}H NMR (300 MHz, $CDCl_3$)**: δ 0.93 (s, 3H), 1.08 (s, 3H), 2.13–2.39 (m, 7H), 3.62 (s, 3H), 5.03 (s, 1H), 6.21 (s, br, 1H), 7.19 (d, *J* = 8.4 Hz, 2H), 7.33 (d, *J* = 8.4 Hz, 2H); **^{13}C NMR (75 MHz, $CDCl_3$)**: δ 19.4, 27.1, 29.4, 32.7, 36.0, 41.1, 50.6, 51.0, 105.3, 111.8, 119.8, 129.6, 131.0, 143.9, 145.8, 148.1, 167.6, 195.4.

Methyl 4-(4-fluorophenyl)-2,7,7-trimethyl-5-oxo-1,4,5,6,7,8-hexahydroquinoline-3-carboxylate (6e)[73]

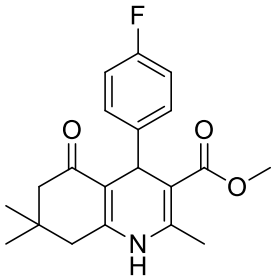

Yellow solid; m.p.: >220 °C (Lit. m.p.: 235–238 °C); **^{1}H NMR (300 MHz, DMSO–d_6)**: δ 0.81 (s, 3H), 0.99 (s, 3H), 2.00-2.49 (m, 7H), 3.51 (s, 3H), 4.85 (s, 1H), 7.00 (t, *J* = 8.7 Hz, 2H), 7.12–7.17 (m, 2H), 9.14 (s, br, 1H); **^{13}C NMR (75 MHz, DMSO–d_6)**: δ 18.2, 26.3, 29.0, 32.1, 35.0, 50.1, 50.6, 103.0, 109.8, 114.4 (d, *J* = 20.7 Hz), 117.6, 128.9 (d, *J* = 7.7 Hz), 143.6, 145.5, 149.5, 167.1, 194.3; HRMS–ESI (*m/z*) calcd for $C_{20}H_{22}FNO_3$ $[M + H]^+$ 344.1662 found 344.1672.

Methyl 2,7,7-trimethyl-4-(3-nitrophenyl)-5-oxo-1,4,5,6,7,8-hexahydroquinoline-3-carboxylate (6f)[43]

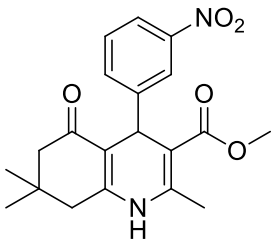

Yellow solid; m.p.: 174–176 °C (Lit. m.p.: 175–176 °C); **^{1}H NMR (300 MHz, $CDCl_3$)**: δ 0.93 (s, 3H), 1.08 (s, 3H), 1.20 (t, *J* = 7.2 Hz, 3H), 2.06–2.42 (m, 7H), 4.07 (q, *J* = 7.2 Hz, 2H), 5.16 (s, 1H), 6.91 (s, br, 1H), 7.38 (t, *J* = 7.8 Hz, 1H), 7.72 (d, *J* = 7.8 Hz, 1H), 7.98 (d, *J* = 8.1 Hz, 1H), 8.13 (s, 1H); **^{13}C NMR (75 MHz, $CDCl_3$)**: δ 14.1, 19.3, 27.0, 29.3, 32.7, 37.0, 40.7, 50.5, 60.0, 104.9, 111.0, 121.2, 122.8, 134.7, 144.7, 148.1, 149.2, 149.4, 167.0, 195.7.

Methyl 4-(3-hydroxyphenyl)-2-methyl-5-oxo-1,4,5,6,7,8-hexahydroquinoline-3-carboxylate (6g)

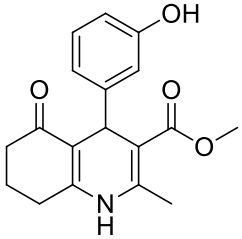

Yellow solid; m.p.: 218–220 °C; **^{1}H NMR (300 MHz, DMSO–d_6)**: δ 1.78–1.98 (m, 3H), 2.20 (s, 3H), 2.24–2.27 (m, 3H), 3.61 (s, 3H), 4.85 (s, 1H), 6.42–6.47 (m, 1H), 6.55–6.58 (m, 2H), 6.89–7.08 (m, 1H), 9.08–9.16 (m, 1H), 9.43 (s, br, 1H); **^{13}C NMR (75 MHz, DMSO–d_6)**: δ 21.2, 26.8, 35.5, 37.2, 51.1, 103.6, 111.5, 112.9, 114.7, 118.3, 129.0, 129.1, 145.4, 149.3, 151.6, 157.4, 167.9, 195.1.

I.C.5.8 Scanned copies of ^{1}H, ^{13}C NMR and HRMS spectra of a representative compound (6c)

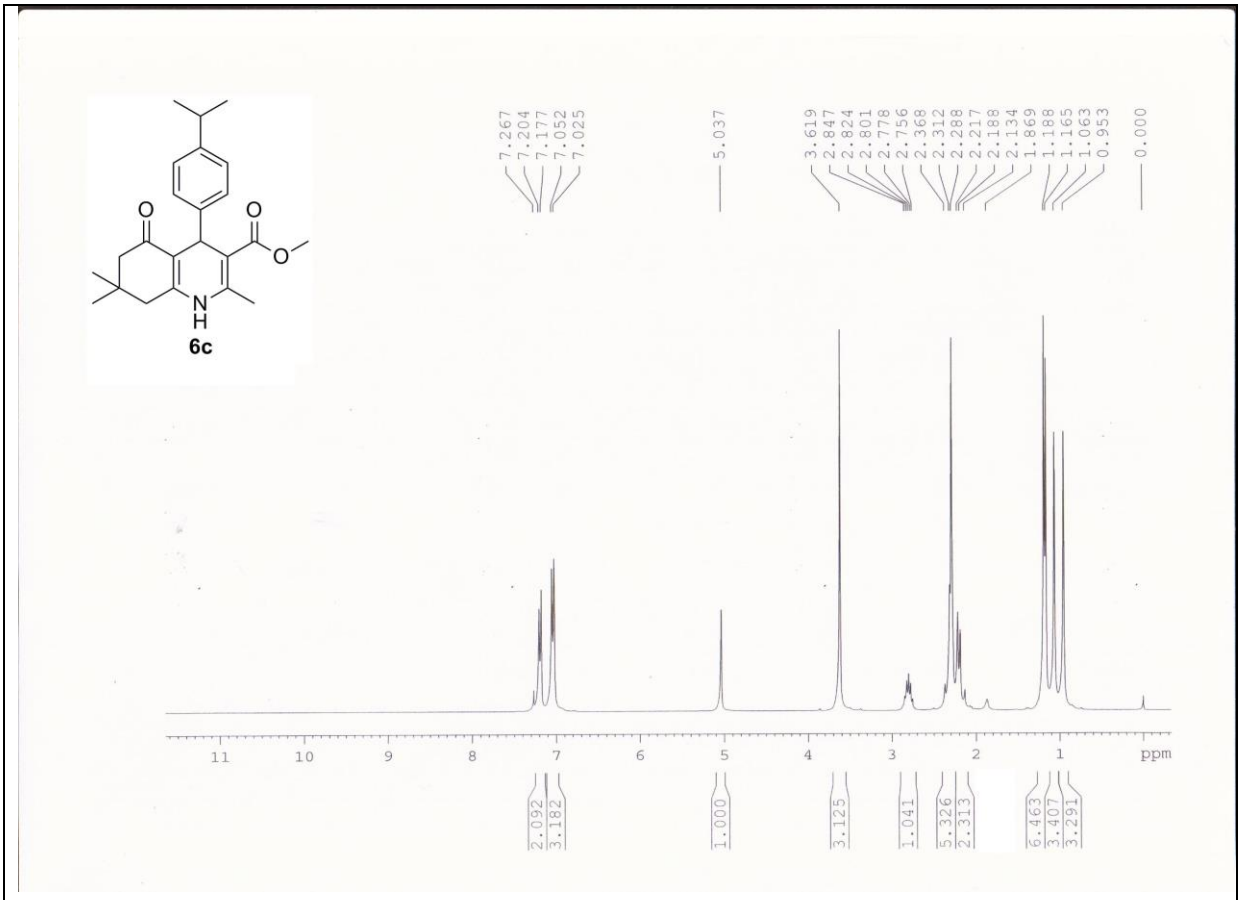

Figure I.C.12 Scanned copy of ^{1}H NMR spectrum of methyl 4-(4-isopropylphenyl)-2,7,7-trimethyl-5-oxo-1,4,5,6,7,8-hexahydroquinoline-3-carboxylate **(6c)**

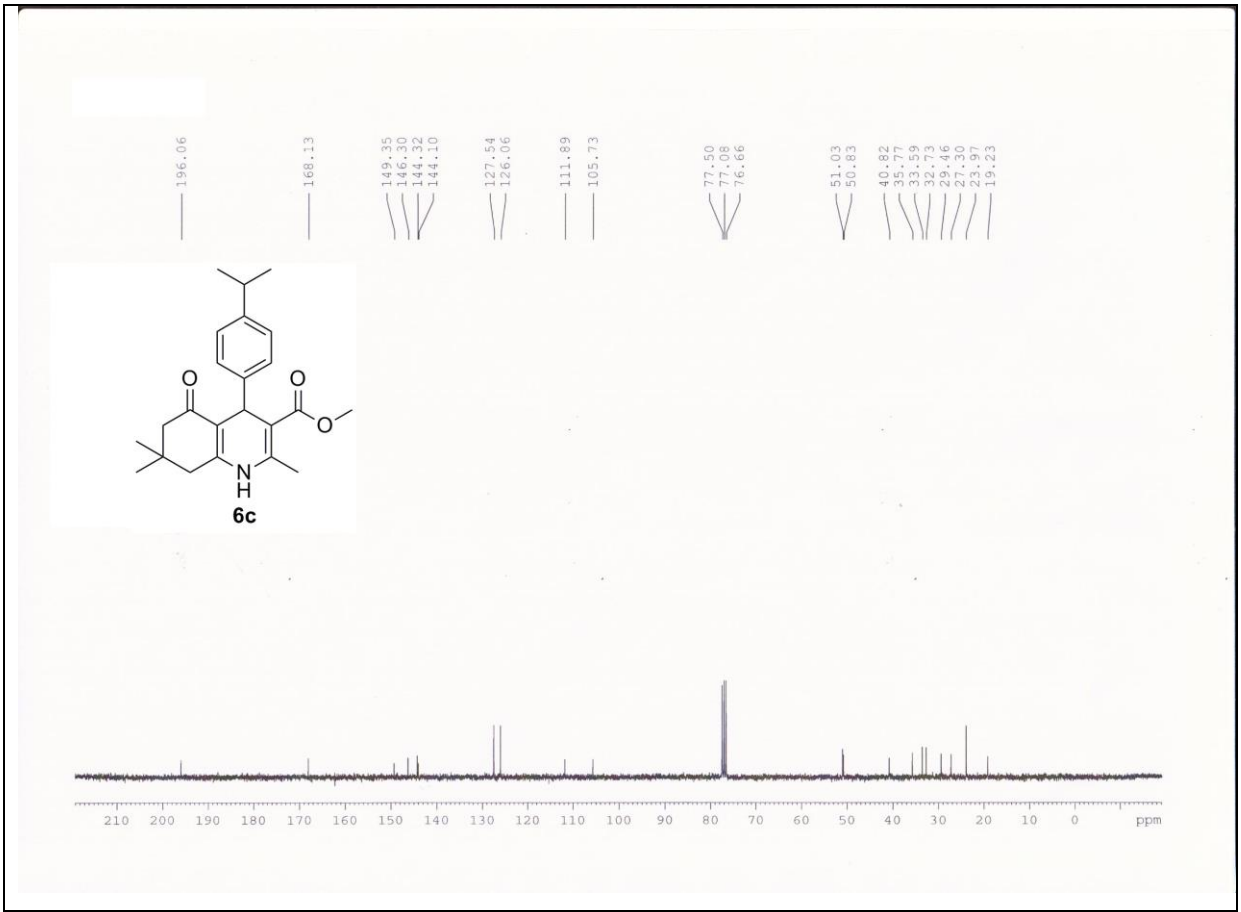

Figure I.C.13 Scanned copy of ^{13}C NMR spectrum of methyl 4-(4-isopropylphenyl)-2,7,7-trimethyl-5-oxo-1,4,5,6,7,8-hexahydroquinoline-3-carboxylate **(6c)**

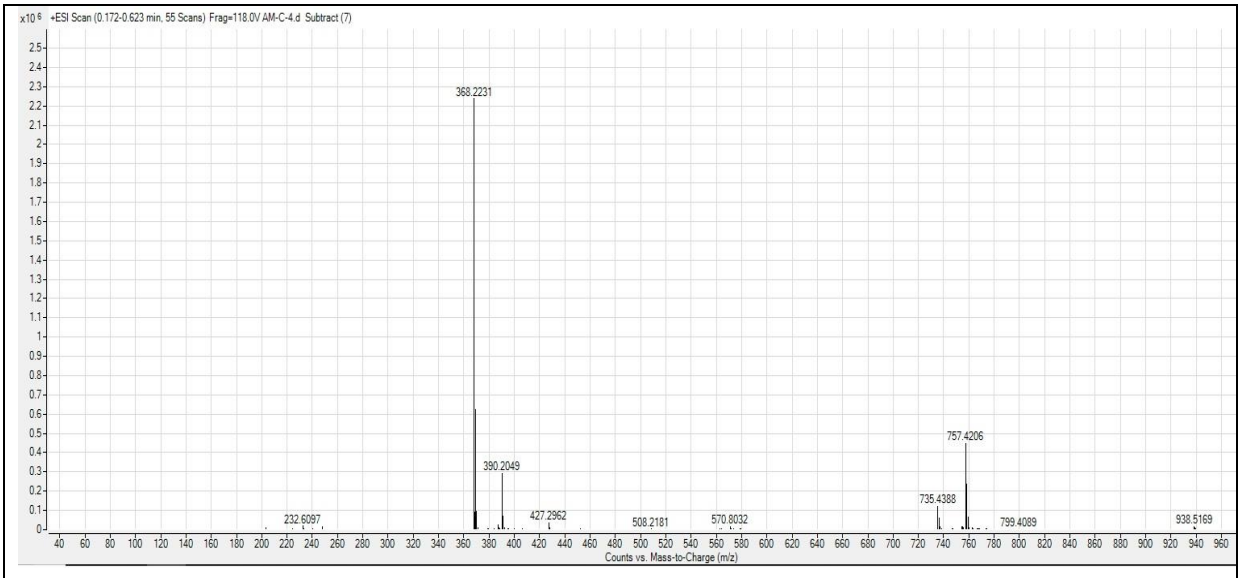

Figure I.C.14 Scanned copy of HRMS spectrum of methyl 4-(4-isopropylphenyl)-2,7,7-trimethyl-5-oxo-1,4,5,6,7,8-hexahydroquinoline-3-carboxylate **(6c)**

I.C.6 References

References are given in BIBLIOGRAPHY under Chapter I, Section C.